Alma Mater Studiorum Università di Bologna
Archivio istituzionale della ricerca

Singular dynamics and emergence of nonlocality in long-range quantum models

(Article begins on next page)

06 May 2024

Rights / License:

Singular dynamics and emergence of nonlocality in long-range quantum models

L. Lepori,[1, *] A. Trombettoni,[2, 3] and D. Vodola[4]

[1]*Dipartimento di Fisica e Astronomia, Università di Padova,Via Marzolo 8, I-35131 Padova, Italy*
[2]*CNR-IOM DEMOCRITOS Simulation Center, Via Bonomea 265, I-34136 Trieste, Italy*
[3]*SISSA and INFN, Sezione di Trieste, Via Bonomea 265, I-34136 Trieste, Italy*
[4]*icFRC, IPCMS (UMR 7504) and ISIS (UMR 7006), Université de Strasbourg and CNRS, Strasbourg, France*

We discuss how nonlocality originates in long-range quantum systems and how it affects their dynamics at and out of the equilibrium. We focus in particular on the Kitaev chains with long-range pairings and on the quantum Ising chain with long-range antiferromagnetic coupling (both having a power-law decay with exponent α). By studying the dynamic correlation functions, we find that for every finite α two different behaviours can be identified, one typical of short-range systems and the other connected with locality violation. The latter behaviour is shown related also with the known power-law decay tails previously observed in the static correlation functions, and originated by modes – having in general energies far from the minima of the spectrum – where particular singularities develop as a consequence of the long-rangedness of the system. We refer to these modes as to "singular" modes, and as to "singular dynamics" to their dynamics. For the Kitaev model they are manifest, at finite α, in derivatives of the quasiparticle energy, the order of the derivatives at which the singularity occurs is increasing with α. The features of the singular modes and their physical consequences are clarified by studying an effective theory for them and by a critical comparison of the results from this theory with the lattice ones. Moreover, a numerical study of the effects of the singular modes on the time evolution after various types of global quenches is performed. We finally present and discuss the presence of singular modes and their consequences in interacting long-range systems by investigating in the long-range Ising quantum chain, both in the deep paramagnetic regime and at criticality, where they also play a central role for the breakdown of conformal invariance.

I. INTRODUCTION

The study of systems with long-range (LR) interactions, both at and out of the equilibrium, gained in the last years an increasing interest [1]. LR interacting quantum systems have been shown in particular to exhibit various peculiar features stemming from the occurrence on nonlocal properties [2–17], including static correlation functions with hybrid (exponential and algebraic) decay [18–21], violation of the area law for the von Neumann entropy (VNE) [19, 20, 22, 23] and possible dominance of multipartite entanglement [24], nonlinear growth for VNE after quenches [25], new constraints on thermalization [13], breakdown of conformal symmetry [26].

Even more interestingly, very recent works [16, 20, 21, 26–29] have shown that LR systems can host new phases at very small values for α, in some cases topological and/or bounded by continuous transition lines where the mass gap does not vanish. These phases are typically signaled by the mentioned violation of the area law for the VNE and/or in some cases by massive edge modes when defects are included. The understanding of the physical origin of these new phases, both at and out of equilibrium, is still incomplete.

Beyond the theoretical activity, an important step forward is coming from experiments. Indeed recently developed technologies in atomic, molecular and optical systems (as polar molecules, Rydberg atoms, trapped ions, magnetic and electric dipoles and multimode cavities) pave the way to the experimental investigation of the mentioned properties [30–48]. For instance paradigmatic LR spin chains, as Ising and XXZ ones, have been experimentally realized with interactions tunable in the strength and in the exponent of their decay with the spatial distance.

Concerning non-equilibrium dynamics, a relevant issue for LR systems is how a certain perturbation, global or local, affects the various parts of the system during the time evolution. A related question, deeply interesting also the equilibrium physics of LR systems, is whether and how the notion of locality is still definable in them and how it evolves as the long-rangedness is varied. For SR lattice quantum models it has been shown long ago that locality is encoded in a bound, called Lieb-Robinson bound [49], for the commutator of two operators defined in different lattice points. This result relies on the existence of a maximum speed propagation for a signal and of a related linear light-cone limiting the causally connected regions in the dynamic correlation functions, up to exponentially small deviations. Moreover it constrains the static correlations to decay exponentially in massive regimes. When LR terms are included in the Hamiltonian, the situation changes drastically. Indeed various papers [4, 9, 10, 19, 46, 47] showed that in these cases the Lieb-Robinson bound is violated. Similar conclusions have been achieved

---

*correspondence at: llepori81@gmail.com

also in classical models, where counterparts of the same bound can be defined [5]. Extensions of the Lieb-Robinson bound have been proposed [2, 6–8, 15], also in the presence of initial entanglement [12], along the last years. The new bounds also allows for the mentioned power-law decay tails in the static correlations, suggesting a close correspondence between the behaviours of static and dynamic physical quantities. Considering the wide generality and model independence of these new bounds, a goal of the present paper is to shed light on their precise dynamic origin.

The open issue to characterize (non)locality in LR systems deserves attention also close to their critical points, where some continuous effective theories (ET) can be constructed by RG approaches. For these theories locality reflects in the Lorentz invariance of their actions, a feature generally emerging close to criticality for SR models [50]. Indeed exactly at criticality this symmetry is implied by conformal invariance, moreover general perturbations, even relevant, of the critical points to massive regimes do not spoil it, although conformal symmetry gets broken. This is for instance the case of the quantum Ising chain in a transverse magnetic field with non critical strength. In the presence of Lorentz invariance a absolute notion of locality is induced, meaning that, given two arbitrary points of the continuous space-time, it is possible to establish without ambiguities if these points are causally connected: causality between them exists, valid in every inertial reference frame, when the points are separated by a time-like distance. As for the Lieb-Robinson bound for lattice models, Lorentz invariance constrains static correlation functions to decay exponentially in massive regimes. This fact suggests a breakdown of it in critical LR systems. In the light of the deep role played by the Lorenz invariance in (SR) critical systems, the naturally arising questions are how Lorentz and conformal invariance disappear in critical LR systems, if some remnants of Lorentz locality survive and how they affect the physical observables. A related question, also motivated by the recent intensive efforts to extend the Lieb-Robinson bound, is how possible symmetries deriving from Lorentz invariance translate at the lattice level.

In the present paper we address these open issues, concerning both the equilibrium and non-equilibrium dynamics. In particular we aim to identify and characterize in detail the origin of the described deviations in LR quantum models from the corresponding SR behaviours. For this purpose, in our investigation we focus at the beginning on a quadratic LR model, the LR paired Kitaev chain [20]. We decided to study this model since its static correlations are known [20, 21, 26], providing a firm basis for the study of its non-equilibrium dynamics: at every α the hybrid decay for static correlations has been derived analitically and the algebraic decay tails have been put in correspondence with a set of states, in general not located close to the minima of the energy spectrum, where divergences arise, in the derivatives of the energy spectrum itself. These divergences are directly related with the presence of LR Hamiltonian terms. The same set of states has been found responsible for the breakdown of conformal symmetry at criticality, as well as of the effective Lorentz invariance at criticality, realized instead in the SR limit [26]. Still in the critical regime, their physical effects have been clarified by a suitable ET for them. In the following of the paper, these states will be denoted "singular modes", and their dynamics as "singular dynamics".

In the light of these results, it is highly interesting to evaluate to what extent singular modes affect the non-equilibrium evolution, making a direct relation with the breakdown of locality. For this purposes, we consider primarily dynamic quantities, as dynamic correlation functions or as the spreading of the information after quenches. We work both at the lattice level and in the continuous limit, exploiting the mentioned ET. Strictly speaking, the ET makes sense only close to the massless lines $\mu = \pm 1$, where it has been derived, however it reveals useful to understand the main features of the singular modes also far from criticality. As outlined in the text, the mentioned dynamic correlations reveal close links with the peculiar features affecting the equilibrium physics. In particular the set of singular modes gives also rise, at every finite α, to non conic causally connected zones in them, as well as to deviations from the conic-like picture predicted by the Lieb-Robinson bound for the spreading of information.

We notice that other recent papers [9, 17, 51] outlined correctly the importance for the non-equilibrium evolution of the divergences in the quasiparticle velocities and/or energies occurring at small enough values for α. However the role of divergences in higher-order derivatives at every finite α has been so far not discussed, as well as the deep links between the LR peculiarities in the equilibrium and non-equilibrium dynamics, for instance concerning the loss of locality.

The central relevance of the singular modes for the LR paired Kitaev chain, as well for the mentioned family of quadratic Kitaev-like Hamiltonians containing it [21], leads to ask if a similar singular mechanism can interest other models, even interacting and having higher dimensionality. In order to deal with this issue, in the final part of the paper we focus on the antiferromagnetic LR Ising chain, inferring the emergence of states encoding singularities both in the paramagnetic limit and close to the critical points, analyzing their effects on some static and dynamic quantities.

The paper and the results presented are organized as follows. The central parts of the discussion are Sections V, VI and VII. In Section II we define the models we are going to consider, while in Section III the main features of the LR Kitaev chains are recalled, both on the lattice chain model and on the ET describing its properties close to the critical lines. In particular the role of the singular modes for the appearance of the LR behaviour is introduced and analyzed. In Section IV, a general discussion is given on the emergence of nonlocality in LR models, both at the lattice level and for the ET. In the second case we find that, although without Lorentz invariance, at every finite α, a reference frame-independent notion of locality does not exist, nevertheless in the presence of a finite maximum quasiparticle velocity a reference frame depending residual notion of locality can be still defined. Finally, the lack of Lorentz locality in LR critical systems is put in direct relation with the possible violation of the Mermin-Wagner theorem in them. In Section V, focusing on the LR paired Kitaev chain, we analyze in detail the evolution

of nonlocality as α is varied, both at the lattice level and using the ET to single out the contribution by the singular modes. A critical comparison between the two approaches is finally made. In particular all the nonlocality related features encountered in the lattice calculations are found correctly reproduced, at least qualitatively, by the ET. This remarkable fact confirms the reliability of the ET to describe the singular dynamics, also when the time evolution is concerned. In Section VI, working again on the LR paired Kitaev chain, we consider the non-equilibrium time evolution on the lattice, analyzing how nonlocality reflects on it and the direct effect by the singular modes. To keep the widest generality as possible, we consider various types of global quenches, from small to large. In particular, at the beginning the overlaps between the pre-quench state and the post-quench excited one are analyzed, giving analitical expressions for them. A critical comparison with the dynamics from the ET is also performed, analyzing the necessary conditions for the ET to describe the time evolution after a small quench to a massless line. For large quenches we perform the analysis of a functional $I(v)$ encoding the relative weights for the velocities v of the states involved in the post-quench dynamics. A discussion of the comparison with recent results [17] is also presented. We also show that $I(v)$ allows to interpolate between the two limits of small and large quenches. The intermediate regime is illustrated better by numerical calculations for the spreading of the mutual information. Finally similarities between the LR and the SR Kitaev chains are inferred, due to the limited effects by the singular modes on the non-equilibrium dynamics, also at very small α. In Section VII we extend the scenario obtained for the LR paired Kitaev chain, especially concerning the role of the singular modes, to the LR Ising chain. We focus at first in the deep paramagnetic limit, where a spin wave approach reveals qualitatively reliable, leading to an Hamiltonian with LR pairing and hopping, as the ones described in [21]. We argue that again an hybrid behaviour is visible at every finite α in the dynamic correlation functions, the non-conic behaviour being ascribable again to the action of the singular modes. Afterwards, we investigate the possible presence of these states far from the deep paramagnetic limit, showing that the distribution of the lowest energy states at criticality is the same of the one for the critical SR Ising model. Then the emergence of the main LR critical features, the breakdown of the conformal symmetry [26] and the effective Lorentz invariance is inferred again related with the action of some higher energy states, as for the LR Kitaev chain at $\mu = 1$. These results suggest that the picture based on singular modes and analyzed into details for the LR paired Kitaev chain can have a wider generality, also including interacting models. Future perspectives, also involving the latter topic, are finally discussed in Section VIII.

II. THE MODELS

In this Section we define the models we investigate in the following of the paper.

A. Long-range paired Kitaev chain

The first model that we consider is the Kitaev Hamiltonian with LR pairing [20] defined on a 1D lattice:

$$H_{\text{lat}} = -w \sum_{j=1}^{L} \left(a_j^\dagger a_{j+1} + \text{h.c.} \right) - \mu \sum_{j=1}^{L} \left(n_j - \frac{1}{2} \right) + \frac{\Delta}{2} \sum_{j=1}^{L} \sum_{\ell=1}^{L-1} d_\ell^{-\alpha} \left(a_j a_{j+\ell} + a_{j+\ell}^\dagger a_j^\dagger \right) . \tag{1}$$

In Eq. (1), a_j is the operator destroying a (spinless) fermion in the site $j = 1, \cdots, L$, being L the number of sites of the chain. For a closed chain, we define $d_\ell = \ell$ ($d_\ell = L - \ell$) if $\ell < L/2$ ($\ell > L/2$) and we choose anti-periodic boundary conditions [20]. Without affecting qualitatively the results given in the next Sections, we set $\Delta = 2w$; furthermore we measure energies in units of $2w$ and lengths in units of the lattice spacing d.

The spectrum of excitations of Eq. (1) is obtained via a Bogoliubov transformation and it is given by

$$\lambda_\alpha(k) = \sqrt{(\mu - \cos k)^2 + f_\alpha^2(k + \pi)} . \tag{2}$$

In Eq. (2), $k = -\pi + 2\pi (n + 1/2) / L$ with $0 \le n < L$ and $f_\alpha(k) \equiv \sum_{l=1}^{L-1} \sin(kl)/d_\ell^\alpha$. The functions $f_\alpha(k)$ can be also evaluated in the thermodynamic limit [21, 26], where they become polylogarithmic functions [52–54].

The spectrum in Eq. (2) displays a critical line at $\mu = 1$ for every α and a the critical semi-line $\mu = -1$ for $\alpha > 1$. Moreover, it is straightforward to show that if $\mu \neq -1$ the velocity of quasiparticle in $k = \pm\pi$ diverges if $\alpha \le \frac{3}{2}$, while it diverges at $\alpha \le 2$ if $\mu = -1$ [20].

The ground state of Eq. (1) is given by $|\Omega\rangle = \prod_{n=0}^{L/2-1} \left(\cos\theta_{k_n} - i \sin\theta_{k_n} a_{k_n}^\dagger a_{-k_n}^\dagger \right) |0\rangle$, defined with $\tan(2\theta_{k_n}) = -f_\alpha(k_n + \pi)/(\mu - \cos k_n)$ and it is even under the Z_2 symmetry, also proper of the Hamiltonian (1), connected with the parity of the fermionic number (see, e.g., [50, 55]). The ground state energy density $e_0(\alpha, L)$ is given by the expression $e_0(\alpha, L) = -\sum_k \lambda_\alpha(k)/(2L)$. We remind that no Kac rescaling [1] is needed for the LR paired Kitaev Hamiltonian of Eq. (1), since $e_0(\alpha, L)$ stays finite in the $L \to \infty$ limit for every values of α, also smaller than 1 [26].

In the limit $\alpha \to \infty$ one recovers the SR Kitaev chain [56]. As it is well known, the latter model can be mapped via Jordan-Wigner transformations to the SR Ising model in transverse field [57]. Below $\alpha = 1$ and at every values of μ, new phases arise. In this regime the area law for the von Neumann entropy is logarithmically violated. Moreover the Majorana fermions, present above $\alpha = 1$ if $|\mu| < 1$, become massive and disappear. Notably the transition to the new phases at $\alpha = 1$ occurs without any mass gap closure, as consequence of the large space correlations induced by the LR pairing [20, 21].

We mention finally that a generalization of the Hamiltonian in Eq. (1), involving also LR hoppings with decay exponent β, can be also defined [21]:

$$H_{\text{lat}} = -w \sum_{j=1}^{L} \sum_{\ell=1}^{L-1} d_\ell^{-\beta} \left(a_j^\dagger a_{j+l} + \text{h.c.} \right) - \mu \sum_{j=1}^{L} \left(n_j - \frac{1}{2} \right) + \frac{\Delta}{2} \sum_{j=1}^{L} \sum_{\ell=1}^{L-1} d_\ell^{-\alpha} \left(a_j a_{j+\ell} + a_{j+\ell}^\dagger a_j^\dagger \right) . \tag{3}$$

This Hamiltonian displays qualitatively equal results compared to the one in Eq. (1).

B. Long-range anti-ferromagnetic Ising chain

The Hamiltonian of the LR Ising antiferromagnetic chain reads:

$$H_{\text{LRI}} = \sin\theta \sum_{i=1;j>i}^{L} \frac{\sigma_i^x \sigma_j^x}{|i-j|^\alpha} + \cos\theta \sum_{i=1}^{L} \sigma_i^z . \tag{4}$$

As usual, σ_j^ν ($\nu = x, y, z$) are the Pauli matrices for a spin-1/2 at the site j on a chain with length L. The first term on the right hand side of Eq. (4) describes LR spin-spin interactions. The second term describes instead the coupling of individual spins to an external field pointing in the z-direction.

In the limit of SR interactions (i.e., for $\alpha \to \infty$) the Hamiltonian in Eq. (4) is exactly solvable and a quantum phase transition is known to occur at $\theta_c = \pi/4$ between a paramagnetic and an antiferromagnetic phases.

We focus in particular on the antiferromagnetic regime for $\sin\theta > 0$ (or equivalently $0 < \theta < \pi$). For a general value of the parameter θ in this range the Hamiltonian in Eq. (4) can be studied only numerically [19, 21].

In Ref. [19], the study of the von Neumann entropy around the space of parameters $0 < \theta < \pi$ and $\alpha > 0$ has shown that a quantum phase transition, separating the antiferromagnetic and the paramagnetic phases, survives for all the finite $\alpha \gtrsim 0.5$.

At variance, below this approximate threshold, a new phase arises on the paramagnetic side, bounded by a transition with non vanishing mass gap and characterized by edge localization of the lowest massive bulk states occurring at higher values of α [21]. Therefore unexpected massive edge states appear. Moreover, a logarithmic violation of the area law for the von Neumann entropy has been found approximately in the same range. The situation is overall similar to the one recalled in the previous Sections for the LR Kitaev Hamiltonians in Eqs. (1) and (3) [21].

III. EMERGENCE OF SINGULAR DYNAMICS IN THE LONG-RANGE PAIRED KITAEV CHAIN

In this Section we analyze the origin of the LR features displayed by the chain in Eq. (1), identifying it in the action of the singular modes at the edge of the Brillouin zone.

An effective description for these modes, particularly important close to the critical lines, is also presented.

A. Lattice correlation functions

In all the phase diagram outside the critical (semi-)lines, the models in Eqs. (1) and (3) are characterized by static correlation functions with a hybrid decay, exponential at short distances and algebraic at larger ones [20, 21].

This decay has been found for other LR models, also interacting as the LR Ising model in Eq. (4) [18, 19, 21], and it looks a general property for such systems.

Due to the solvability of the model in Eq. (1), the origin of the hybrid decay can be followed directly: in [21, 26] it has been considered for instance the static correlation function

$$g_1^{(\text{lat})}(R) \equiv \langle a_R^\dagger a_0 \rangle . \tag{5}$$

It has been found that the main contribution giving rise to the exponentially decaying part comes from the modes close to the minimum of the energy spectrum, $k \approx 0$, while the algebraic tail is mainly due to the action of the modes close to the edges

of the Brillouin zone, $k \approx \pi$. Similar features occur for the anomalous correlation $g_{1\,(\mathrm{an})}^{(\mathrm{lat})}(R) \equiv \langle a_R^\dagger a_0^\dagger \rangle$ and for every other n-points static correlations, that can be obtained from $g_1^{(\mathrm{lat})}(R)$ and $g_{1\,(\mathrm{an})}^{(\mathrm{lat})}(R)$ by the Wick theorem.

The modes close to $k = \pi$ display singularities at every finite value for α. More in detail, if $\alpha > 2$ or $\alpha < \frac{3}{2}$ (and apart from the peculiar case $\mu = -1$), they occur in the $[\alpha]$-th k-derivative of the energy spectrum $\lambda(k)$, $[\alpha]$ denoting the integer part of α, while in the second derivative if $\frac{3}{2} < \alpha < 2$. For this reason we call them "singular modes" and their dynamics "singular dynamics".

In the next Sections these modes will be argued responsible of the non SR behaviour of the Hamiltonian in Eq. (1). For instance the hybrid behaviour of the correlations, together with its relation with the modes close to $k = \pi$, leads directly to identify the origin of the violation the Lieb-Robinson bound [2, 6, 8], required by the hybrid decay itself, in these eigenstates.

B. Singular dynamics close to criticality

In Ref. [26] an ET has been derived by an RG approach close to the critical lines $\mu = \pm 1$. It has been found that this ET is able to prove directly the breakdown of conformal symmetry on the critical lines for $\alpha < 2$, as well as the violation of the area law for the von Neumann entropy below $\alpha < 1$.

1. Critical line $\mu = 1$

Close to $\mu = 1$ the effective action

$$S = S_{\mathrm{D}} + S_{\mathrm{AN}}^{(\alpha \gtrless 2)}, \tag{6}$$

was recognized to be composed by two commuting contributions, corresponding to the two sets of states responsible for the hybrid behaviour of the static correlations: the action S_{D}, originated from the modes close to the minimum of the spectrum ($k \approx 0$), as common in SR systems, and the anomalous action S_{AN} coming from the high-energy singular modes at the edges of the Brillouin zone ($k \approx \pi$).

The origin of S_{AN} is that, along the renormalization procedure leading to the ET, one has to avoid to integrate out the singular modes, such not to end up with a non smooth RG flow [26] because of their divergences.

More in detail, S_{D} is the Euclidean Dirac action, massless at criticality, while S_{AN} reads for $\alpha > 2$

$$S_{\mathrm{AN}}^{(\alpha>2)} = \int \mathrm{d}x\,\mathrm{d}\tau \left\{ \bar{\psi}_{\mathrm{H}}(\tau,x)\,\gamma_0\,\partial_\tau\,\psi_{\mathrm{H}}(\tau,x) + \bar{\psi}_{\mathrm{H}}(\tau,x)\big[\gamma_1\left(\partial_x + \cdots + a(\beta)\,\partial_x^\beta\right) + M\big]\,\psi_{\mathrm{H}}(\tau,x) \right\} \tag{7}$$

and for $\alpha < 2$

$$S_{\mathrm{AN}}^{(\alpha<2)} = \int \mathrm{d}x\,\mathrm{d}\tau\,\bar{\psi}_{\mathrm{H}}(\tau,x) \left(\gamma_0\,\partial_\tau + \gamma_1\,\partial_x^\beta + M \right)\psi_{\mathrm{H}}(\tau,x). \tag{8}$$

In Eq. (8), $\gamma_0 = -\sigma_3$, $\gamma_1 = -i\,\sigma_1$, $\beta \equiv \alpha - 1$ and the notation using the fractional derivative means that the inverse propagator of the effective action in Fourier space depends on p^β, $p \equiv k - \pi$. Moreover in Eq. (7), $a(\beta) \ll 1$ and the dots denote odd n-th derivatives with $n < \beta$: the effect of these integer derivatives on the dynamics is found qualitatively negligible [26], opposite to the term $\propto \partial_x^\beta$. The Hamiltonian related to the action in Eq. (8) reads in momentum space [26]:

$$H_{\mathrm{AN}} = \int \mathrm{d}p\,\bar{\psi}_{\mathrm{H}}(p)\left[\gamma_1\,p^\beta + M\right]\psi_{\mathrm{H}}(p). \tag{9}$$

The hermiticity of this Hamiltonian is manifest, guaranteeing the unitarity of the corresponding free field theory.

An important point to be stressed is that the action in Eq. (8) for $\alpha < 2$ is an nonlocal ET, unlike the case $\alpha > 2$ for which the action in Eq. (7) is local. The nonlocal ET for the quantum LR Kitaev models has been derived in [26] exploiting the solvability of the model, while a nonlocal ET to study $O(N)$ LR classical models have been recently used both for isotropic [58] and anisotropic [59] LR couplings, retrieving the Sak results for the critical exponents [60], in agreement with very recent Monte Carlo simulations [61]. We introduce here the action in Eq. (8) since we intend to compare the results of the lattice LR Kitaev model and its nonlocal properties for $\alpha < 2$, with the findings of an effective continuous theory close to the critical lines, that should be necessarily nonlocal. Our results indicate that the ET qualitative reproduces for $\alpha < 2$ the emergence of nonlocal properties in the lattice theory, even though it does not completely reproduce the light-cone structure for large distances. The reason of this secondary mismatch will be analyzed in Sections V and VI.

If $\alpha > 2$, exactly at criticality the effective action S is made only by S_{D}, then conformal symmetry is realized, while outside of criticality it has the double contribution as in Eq. (6). However S_{D} is dominant (in the RG sense) against the anomalous
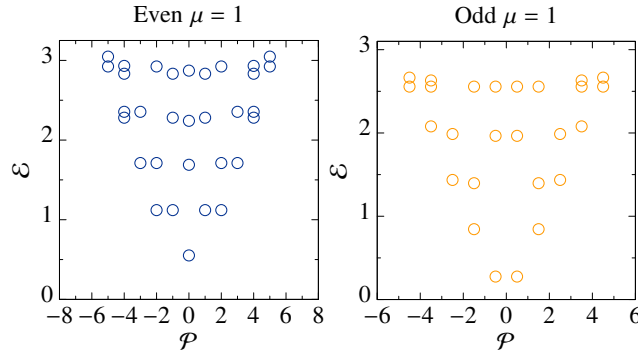
FIG. 1: Distributions of the lowest excited levels for the critical LR paired Kitaev chain in Eq. (1) for $\mu = 1$ and $\alpha = 1.25$. The left panel shows the sector with an even number of quasiparticles. In both the panels the doubly degenerate levels are marked by a double circle. Taking into account also the ground state at zero energy (not plotted), we recognize for the lowest energy eigenstates a distribution in multiplets (all the elements having the same energy, up small finite size effects) along the pattern $1 - 1 - 4 - 5 - 9 - 13$, typical of the SR Ising universality class [63]. In particular these states correspond to the sum of the non chiral conformal families $(0, 0) + \left(\frac{1}{2}, \frac{1}{2}\right)$. Notice that the distance in energy between the multiplets is constant, are required by conformal invariance [50, 62, 63]. The right panel shows instead the sector with odd number of quasiparticles. There again the SR Ising degeneracy patters $2 - 2 - 4 - 6 - 12$ is found, corresponding to the sum of the non chiral conformal families $\left(0, \frac{1}{2}\right) + \left(\frac{1}{2}, 0\right)$.

action S_{AN}. Conversely, if $\alpha < 2$ both at and outside of criticality the effective action has the double contribution as in Eq. (6), however in this case S_{AN} is dominant with respect to S_{D}. At criticality this fact results in the breakdown of conformal symmetry. The same breakdown is also signaled by an anomalous scaling for the ground state energy [20, 21]. Moreover it is not Lorentz invariant any longer, then the total ET looses this feature, typical of the ET governing the critical points for the SR systems [50, 62].

Concerning the mass M in Eq. (7), the study of the RG flow reveals that $M \to \infty$ along it if $\alpha > 1$, while $M \to 0$ if $\alpha < 1$. This change of behaviour signals the previously mentioned quantum phase transition without mass gap closure on the line $\alpha = 1$, moreover it implies a deviation from the area law for the von Neumann entropy below if $\alpha < 1$ [26], as for SR massless system.

We also mention that, as on the lattice, the hybrid decay behaviour of the static correlation functions obtained around criticality from the ET in Eq. (6) is in one-to-one correspondence with the two actions S_{D} and S_{AN} [26].

The central role of the singular modes for the critical dynamics, in particular for the emergence of the effective action S_{AN} breaking conformal invariance at $\alpha < 2$ can be inferred also from the distributions on the lattice of the lowest energy levels, derivable from the quasiparticle spectrum in Eq. (2). In particular it is interesting, also for future convenience, to compare them with the typical distribution of the SR Ising universality class (in the present paper anti-periodic boundary conditions are assumed). This distribution, derived from conformal theory, can be found e.g. in [50, 62], while the results for the Hamiltonian in Eq. (1) is displayed in Fig. 1. There we find that the degeneracies of the SR Ising model [63] are recovered (see the degeneracy pattern in the caption of the same figure) [64], in spite of the breakdown of the conformal invariance at $\alpha < 2$.

Notice that, although in [26] the breakdown of the conformal symmetry has been investigated using a finite-size scaling for the ground-state energy density, the same approach is not able to probe the structure of the lowest energy levels, unlike the approach presented here. The same strategy will be used in Section VII, where similar features as the ones described in the present Section are discussed for the antiferromagnetic LR Ising model.

2. Critical semi-line at $\mu = -1$

A similar ET analysis as the one carried on for $\mu = 1$ can be provided when $\alpha > 1$ for the critical line $\mu = -1$ $\left(\text{for } \alpha < 1 \text{ the Hamiltonian in Eq. (1) acquires a mass gap}\right)$.

Now the minimum of the energy spectrum and the location of the singular states occur at the same momentum $k = \pi$, where the energy dispersion grows linearly for $\alpha > 2$, and as $k^{\alpha-1}$ for $\alpha < 2$. The resulting distribution for the lowest energy levels is plotted, for comparison with Fig. 1, in the Appendix A. As a consequence, at criticality the breakdown of conformal symmetry appears exactly at $\alpha = 2$. Moreover a unique term arises in the effective action S. Indeed if $\alpha > 2$ the same ET as in Eq. (7) is found, again parametrized by m. Conversely if $\alpha < 2$ the ET has the same functional form as in Eq. (8), but with $\beta = \frac{\alpha-1}{2}$. Moreover the same equation is characterized by a mass $m \propto |\mu + 1|$ diverging along the RG flow and vanishing on the critical line, as in S_{D}. Unlike the case $\mu = 1$, in deriving the static correlations from the ET one can show [26] that both their exponentially and algebraically decaying parts take origin from the unique term in S.

IV. BREAKDOWN OF LOCALITY IN LONG-RANGE QUANTUM LATTICES

In order to investigate the issues presented in the Introduction and to highlight the role of the singular modes for temporal evolution, in this Section we first discuss the general concepts of locality and breakdown of it in LR systems. The latter concept and its consequences will be described in more detail on specific models in Sections V, VI, and VII.

A. Nonlocality on LR lattice models

For SR lattice systems the notion of locality is encoded in the Lieb-Robinson bound [49]. This is a theorem stating that, given an operator $O(t, x)$, the inequality $|\langle \mathrm{GS}|[O(t,x), O(0,0)]|\mathrm{GS}\rangle| \lesssim a\, e^{-b(x-v_{\max}t)}$ holds, where a, b and v are model dependent parameters. The Lieb-Robinson bound implies a maximum propagation speed $v_{\max}$ of the excitations, which is at the basis of the definition of locality. Related to $v_{\max}$, a linear light-cone is present limiting the region (t, x) correlated with the starting point $(0, 0)$ of a certain signal. We point out that locality, defined as above, holds up to exponentially small corrections, present also outside of the light-cone.

Related to locality, the Lieb-Robinson bound also implies an exponential decay for the static correlations [2] in the presence of a mass gap, similarly as the Lorentz invariance in the continuous space-time. For this reason the algebraic decay tails in the static lattice correlations, as the ones seen in Section III, are a direct signal for the (power-law) violation of the bound. Notably this violation occurs in the model of Eq. (1) also in the presence of a finite maximum group velocity. Indeed the same violation is related to the singular modes occurring at every finite α, as we are going to discuss.

Extensions of Lieb-Robinson bound in the presence of LR Hamiltonian terms have been recently proposed [2, 6–9, 15], In particular in [8] the following new bound has been derived:

$$|\langle \mathrm{GS}|[O(t,x), O(0,0)]|\mathrm{GS}\rangle| \lesssim a\left(e^{v_{\max}t} - b\,\frac{r}{t^\gamma}\right) + c\,\frac{t^{\alpha\,(1+\gamma)}}{x^\alpha}, \tag{10}$$

α being the exponent associated to the algebraic decay of the interaction between the lattice sites, a, b, and c three non universal multiplicative constants and γ a second exponent to be chosen conveniently.

The bound in Eq. (10) is able to predict in a qualitatively correct way some important features of the static and dynamic correlation functions. In particular it allows for the hybrid decay of the static correlation functions encountered in LR systems and it suggests a similar hybrid behaviour also for dynamic correlations [2, 8], which is the subject of the next Subsections.

Notably it contains two contributions: one remnant of the Lieb-Robinson bound for SR lattice models, and a new one directly connected to the long-rangedness of the studied model. For the LR paired Kitaev chain in Eq. (1) the effect of the singular modes is then expected encoded in the second term of Eq. (10).

B. Nonlocality and relative locality on the continuous space-time

The nonlocality structure described above in LR lattice systems has a direct counterpart for the ET governing their critical dynamics. We illustrate this parallelism using the ET in Eq. (6) for the LR paired Kitaev chain. We remind that out of criticality the effective Lorentz invariance, exact for the total action S in the limit $\alpha \to \infty$ (where S_D just acquires a mass term), is broken at every finite values of α, since S_AN is not Lorentz covariant. Conversely, exactly at criticality the Lorentz group, belonging to the conformal one, is broken only below $\alpha = 2$ [26]. Starting from these observations, we now discuss how nonlocality occurs in non Lorentz invariant ET.

Lorentz invariance, when realized, induces the further notion of (Lorentz) locality, basically related to a finite maximum speed of propagation $v_{\max}$ for a signal, which is of course constant in every inertial reference frame. Indeed under this condition locality is defined, as usual in special relativity, in terms of the invariant interval $\Delta s = \mathrm{d}x^2 + \mathrm{d}\tau^2 = \mathrm{d}x^2 - v_{\max}^2 \mathrm{d}t^2$. All the physical operators (anti-)commute if they are measured at two space-time points with space-like distance, $\Delta s > 0$. It is clear that locality, defined in this way, allows to establish without ambiguities whether two arbitrary points of the space time are causally correlated. Moreover this definition is equivalent to the notion of Lorentz invariance itself [65].

We also notice that in the recent literature on the propagation of signals in LR systems (see [3, 6, 8–10, 14, 46, 47, 67] and reference therein), although locality is correctly put in direct relation with the existence of a maximum speed $v_{\max}$ for a signal, generally no explicit mention is made about the invariance of $v_{\max}$ passing from an inertial reference frame to another one, as required by Lorentz locality. Without this requirement, $v_{\max}$, even if finite, is well defined only after the choice of a particular reference frame, as well as the notion of locality itself. In the following we will quote this weaker locality as *relative locality*.

Strictly speaking, the difference between Lorentz and relative locality is well defined only in a continuous space-time, since only in this condition continuous changes of reference frame are possible. For an ET derived from a LR lattice model, in absence of Lorentz locality, the reference frame where relative locality is defined is the one naturally inherited from the original lattice model. Notice however that, differently from relative locality, Lorentz locality has a natural counterpart on the lattice, encoded in the Lieb-Robinson bound introduced above.

A clear example of the need for distinguishing between Lorentz and relative localities is given by the ET in Eq. (6) for the model in Eq. (1). For $\alpha > \frac{3}{2}$ they are characterized by finite quasiparticle velocities (as it happens on the lattice), even if the effective Lorentz invariance is not realized. In this condition all the velocities are frame-dependent, as well as the causal connection between two points in the $(1+1)$ continuous space-time where the same theories are defined.

We alert the reader that the violation of locality can raise doubts concerning the validity for $\alpha < 2$ of the ET in Eq. (8) itself, since it is known (see e.g. [66]) that a requirement for the consistency of a given field theory is, apart form unitarity (here fulfilled), locality. However for the system in Eq. (1), where the action in Eq. (8) comes from, locality is already violated at the lattice level in the sense specified in Section IV A. This violation indeed is one of the most clear differences with respect to SR lattice models. For this reason, the same violation is present for the corresponding ET in Eq. (8). More in detail, this ingredient has been found required to explain remarkable lattice properties as the breakdown of conformal symmetry exactly at criticality or the hybrid decay for the two points correlation functions in gapped regimes, as recalled in the previous Sections. Other examples of field theories describing correctly critical points of LR lattices can be found e.g. in [14] and [68].

We mention finally that the breakdown of the effective Lorentz invariance at and close to criticality is related with the violation of the Mermin-Wagner theorem [16, 69–71], forbidding the breakdown of a continuos symmetry if the (integer) dimensionality D of the real space is lower than 3 [72, 73]. In $D = 2$ this fact appears particularly clear assuming a Landau-Ginzburg formulation of the considered model close to criticality. There, in the absence of the effective Lorentz invariance (as well as of the conformal invariance exactly at criticality) the Landau-Ginzburg action is generally expected to assume the form [74]:

$$S = \int \mathrm{d}x \, \mathrm{d}t \left[\phi^\dagger(x, \tau)\Big(-\partial_t^2 + \partial_x^\gamma \Big)\phi(x, t) + g \, |\phi(x, t)|^4 \right]. \tag{11}$$

where $\gamma < 2 = D$, such to assure the relevance of the term in ∂_x^γ against the Lorentz one in ∂_x^2 along the RG flow (see Section II and [26]). The scalar field $\phi(x, t)$ describes the massless fluctuations along flat directions of the order parameter O driving the considered phase transition. In this condition the propagator of the theory in Eq. (11) reads:

$$\langle 0|\phi^\dagger(x, t)\phi(0, 0)|0\rangle = \int \frac{dp}{4\pi} \, e^{ipR} \frac{1}{p^\gamma} \left[f_+(p, t) + f_-(p, t) \right], \tag{12}$$

with $f_\pm(p, t) = \theta(\pm t) \, e^{i\sqrt{(p^\beta)^2 + M^2}\, t}$ [26]. This expression is well defined if $\gamma < 2 = D$, allowing for the appearance of finite energy Goldstone bosons, then for the violation of the Mermin-Wagner theorem. The picture described here has been presented for the LR XXZ chain in [16].

V. NONLOCALITY IN THE LR PAIRED KITAEV CHAIN

In this Section we focus on the evolution of nonlocality as α decreases from very large values towards 0 in the LR paired Kitaev chain. We work separately both on the lattice (with Hamiltonian given by Eq. (1)) and using the ET at criticality (with action given by Eq. (6)). A critical comparison between the results in the two limits is performed and the role played by the singular modes is discussed in detail.

A. Lattice results

In this Subsection we investigate lattice (non-)locality for the LR Kitaev chain, as α is varied from ∞ to 0. This can be done analyzing for instance the time dependent correlation function:

$$\Gamma(t, R) \equiv \mathrm{Re} \, \langle 0|\{a_0 \, , \, a_R^\dagger(t)\}|0\rangle. \tag{13}$$

The real part in Eq. (13) has been taken to not assume any temporal order for the anticommutator. This choice is useful for the future comparison of Eq. (13) with its counterpart, Eq. (17), obtained by ET in Eq. (6) (of course again not assuming any time order). Notably $\Gamma(t, R)$, which contains an anticommutator, also allows for a direct comparison with the Lieb-Robinson bound, even if for the latter quantity a commutator is involved. This is possible as all the conceivable physical observables are functions of bilinears of the fermionic fields, involving commutators [75].
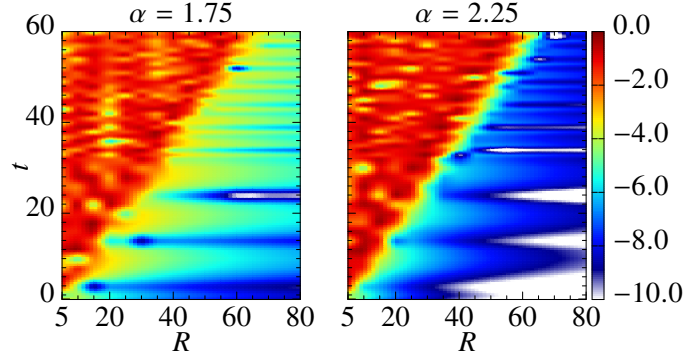
FIG. 2: Plots of $\log\big[\Gamma(t,R)\big]$ in Eq. (13) for $\mu = 0.95$ and $\alpha = 1.75$ (left panel) and $\alpha = 2.25$ (right panel). In every point of the panels the values are normalized with respect to the global maximum of the corresponding panel.
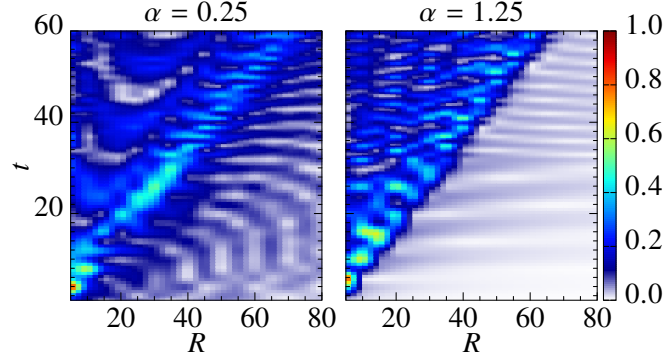

FIG. 3: Plots of $\Gamma(t,R)$, defined in Eq. (13), for $\mu = 0.95$ and $\alpha = 0.25$ (left panel) and $\alpha = 1.25$ (right panel). In each point of the panels the values are normalized with respect to the global maximum of the corresponding panel.

The results are shown in Figs. 2 and 3 for $\mu = 0.95$ and different values of α:

(i) Above $\alpha = 2$ (the case $\alpha = 2.25$ is reported in Fig. 2) a linear light-cone is clearly visible, numerically compatible with a very small violation of the Lieb-Robinson bound, expected to be restored in the limit $\alpha \to \infty$. Such a restoration, as well as the minor deviations from the Lieb-Robinson bound above $\alpha = 2 = D + 1$, has been predicted in general in [6]. However very tiny correlated regions with $\Gamma(t,R) \neq 0$ outside of the conic zone already appear, resembling finite lobes departing from the linear light-cone. The same situation occurs in the range $\frac{3}{2} < \alpha < 2$ (the case $\alpha = 1.75$ is shown), the lobes becoming here more important. Small deviations from the linear cone regime for $\alpha > \frac{3}{2}$ are magnified in Fig. 2 plotting $\log\big[\Gamma(t,R)\big]$ instead of $\Gamma(t,R)$ (as instead for $\alpha < \frac{3}{2}$). Notably these deviations occur in the presence of a finite maximum quasiparticle velocity, already suggesting the role of the higher-order k-derivatives of the quasiparticle dispersion mentioned in Section III. Similar lobes have been found in other lattice models [4].

(ii) For $1 < \alpha \leq \frac{3}{2}$ (the case $\alpha = 1.25$ is reported in Fig. 3), although a linear light-cone is still present, the lobes become more pronounced and start to elongate towards infinity, forming stripe shaped regions [76]. However a totally uncorrelated region remains close to the line $t = 0$. The enlarged extension of the correlated zones out of the cone seems to parallel the divergence of the maximum propagation group velocity $v(k) = \frac{\partial \lambda(k)}{\partial k}$, v_{max}, for the quasiparticles in this regime, even if no drastic change of behaviour is found as v_{max} diverges. This fact is due to the combined action of the entire set of Bogoliubov quasiparticles in the Brillouin zone, as explained in the following.

These results qualitative agree with the new bound in Eq. (10), by which two independent behaviours for the dynamic correlation functions are predicted. In particular a conic region is still present below $\alpha = \frac{3}{2}$, where the maximum quasiparticle velocity diverges. Its origin will be clarified in the next Subsections.

(iii) Finally for $\alpha < 1$ (the case $\alpha = 0.25$ is displayed), although an approximately linear light-cone is still present at sufficiently small values for the ratio $\frac{R}{\tilde{v}\,t}$ (being $\tilde{v}$ an arbitrary finite velocity scale, for instance the one determining the slopes of the conic zone in Fig. 3), for larger values of this ratio the correlation is spread around all the space-time and no uncorrelated regions are remaining (up to numerical finite size effects). This peculiar spread for correlation parallels an instantaneous propagation for signals [3] and it has been argued to be related to the divergence of the quasiparticle energy $\lambda(k)$. We observe that the prediction for the spread of the correlations is a consequence of the nonlocality of the ET in Eq. (8), that has to be contrasted with the results from the lattice, for which the cone is more clearly defined. The origin of this mismatch is the vanishing density of the

singular states at the lattice level, noticed in [17] and recalled in Section VI.

It is important to discuss at this point the origin of the light-cone encountered in Fig. 3. In the discussion in Section III about the ET around the critical line $\mu = 1$, a Dirac part S_{D} of the total action has been isolated, coming from the lowest energy modes at $k \approx 0$ with velocity coinciding with the Fermi velocity $v_F^{(0)}$. At the same time in [17] a peak on the density of states in velocity $\rho(v) = \frac{\partial k(v)}{\partial v}$, extracted from the lattice spectrum, has been found around $v_F^{(0)}$. This peak has been argued to have a dominating effect on the non-equilibrium dynamics of the LR paired Kitaev chain.

These facts lead to think that the cone observed in Fig. 3 has a slope characterized by $v_F^{(0)}$. The latter quantity can be calculated expanding in powers of k the terms under the square root in the lattice energy spectrum in Eq. (2) and selecting the square root of the coefficient in front of the term $\propto k^2$. By direct calculation we obtain

$$v_F^{(0)}(\mu, \alpha) = \sqrt{\mu - 1 + \mathrm{Li}_{\alpha-1}(-1)^2}\,, \tag{14}$$

with μ close to 1. At fixed μ, $v_F(\mu, \alpha)$ decreases monotonically with α going to zero, up to a finite value at $\alpha = 0$. In this way the conic zone shrinks towards the zone close to the line $R = 0$. A numerical fit of the slopes for the cones at various values for α and μ by Eq. (14) is in satisfying agreement with our expectation that $v_F^{(0)}$ characterizes the slope of the light-cone in Fig. 3.

Qualitatively similar results as the ones described above are found close to the massless line $\mu = -1$ and in every range for α. In particular, we remark for future convenience that again both a connected conic zone and another external one with infinite extension are found, having different relative importance as α varies (similar to Fig. 3).

B. Effective description of the singular modes

In the previous Subsection the role played by the singular modes is partly hidden by the contribution of the other modes in the Brillouin zone. Their effect can be isolated by studying the ET described in Section III, indeed taking into account only the singular modes (S_{AN}) and the lowest energy ones (S_{D}). For the same reasons, this study allows to investigate the violation of locality approaching criticality. Strictly speaking, the same ET makes sense only close to the massless lines $\mu = \pm 1$, where it has been derived, however it reveals useful to understand the main features of the singular modes also far from criticality (provided that structure of the spectrum does not change, as interpolating between the critical lines).

We focus at the beginning on $\alpha < 2$ and we work in a $(1+1)$ dimensional Minkowski space. We consider in particular the quantity

$$A(r^\mu) = A_{\mathrm{L}}(r^\mu) + A_{\mathrm{H}}(r^\mu) = |\langle 0|\{\psi_{\mathrm{L}}(x^\mu), \bar{\psi}_{\mathrm{L}}(y^\mu)\}|0\rangle| + |\langle 0|\{\psi_{\mathrm{H}}(x^\mu), \bar{\psi}_{\mathrm{H}}(y^\mu)\}|0\rangle|, \tag{15}$$

with $r^\mu \equiv x^\mu - y^\mu$ and $\psi_{\mathrm{L}}(x^\mu)$ is the fermionic field entering in the Dirac action S_D in Eq. (6). $A_{\mathrm{H}}(r^\mu)$ is related to the singular modes. Unlike $A_{\mathrm{L}}(r^\mu)$, this quantity cannot be obtained directly from the static correlation functions: Eq. (8) breaks Lorentz invariance explicitly, then space-like and space-time correlation functions cannot be linked by Lorentz rotations.

An explicit calculation yields

$$A_{\mathrm{H}}(r^\mu) = \left|\left(i\gamma_0\,\partial_t + (-i)^\beta \gamma_1\,\partial^\beta_{(x-y)} + M\right) B_{\mathrm{H}}(r^\mu)\right|, \tag{16}$$

with

$$B_{\mathrm{H}}(r^\mu) = -i\,\mathrm{Im} \int \frac{\mathrm{d}p}{2\pi} \frac{e^{ip_\mu r^\mu}}{\sqrt{(p^\beta)^2 + M^2}} \tag{17}$$

and $p_\mu \equiv \left(\sqrt{(p^\beta)^2 + M^2}, p\right)$ and $\beta = \alpha - 1$. We notice that $A_{\mathrm{L}}(r^\mu)$ has the same expression as Eqs. (16) and (17) with $\beta = 1$ [75]. In this case $B_{\mathrm{L}}(r^\mu)$ vanishes for space-like separations, since by a Lorentz boost one can map $r^\mu \to -r^\mu$. This situation is depicted in Fig. 6 (b).

However if $\beta \neq 1$, the situation arising at every $\alpha < 2$, Lorentz invariance does not hold any longer and the possible vanishing of $B_{\mathrm{H}}(r^\mu)$ in a point of the space-time is reference frame dependent (then only relative locality, defined in the Subsection IV A, remains). The quantity $A(r^\mu) = A_{\mathrm{L}}(r^\mu) + A_{\mathrm{H}}(r^\mu)$ is the effective analogous of the lattice correlation matrix:

$$\mathrm{Re} \begin{pmatrix} -\langle\{a_0,\,a_R^\dagger(t)\}\rangle & \langle\{a_0^\dagger,\,a_R^\dagger(t)\}\rangle \\ -\langle\{a_0,\,a_R(t)\}\rangle & \langle\{a_0^\dagger,\,a_R(t)\}\rangle \end{pmatrix},$$

as clear from the definition of the Dirac matrices in Section III. In particular $\Gamma(t, R)$ in Eq. (13) corresponds to the terms $\propto M$ and $\propto \gamma_0$ in Eq. (16).
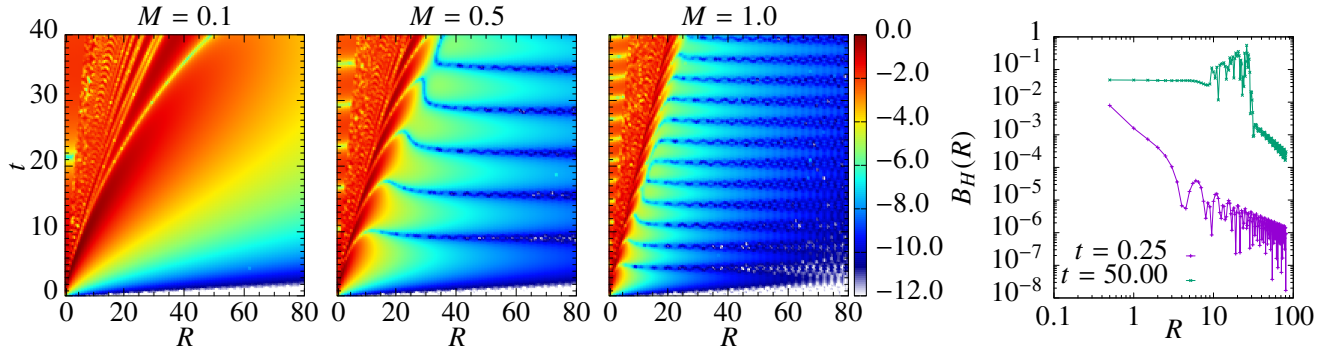
FIG. 4: Three panels on the left: Plots of $\log\left[B_{\mathrm{H}}(r^\mu)\right]$, defined in Eq. (17), for $\alpha = 1.75$ and $M = 0.1$ (left panel), $M = 0.5$ (left central panel) and $M = 1$ (right central panel). In each point of the panels in this Figure and as well in the Figs. 5-6, the values are normalized with respect to the global maximum of the corresponding panel. Right panel: Plots of $B_{\mathrm{H}}(r^\mu)$ for $\alpha = 1.75$, $M = 1$ at the fixed times $t = 0.25$ and $t = 50$ for R varying (two logarithmic scales are used).

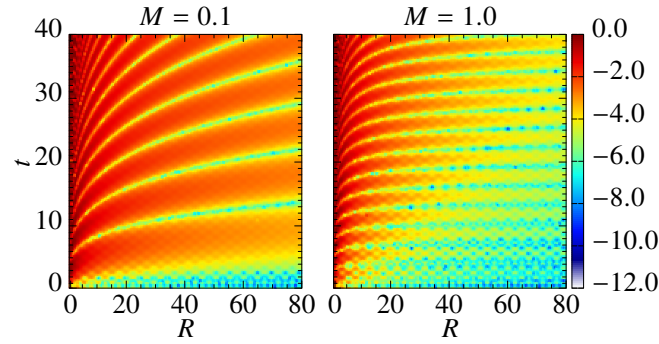FIG. 5: Plots of $B_{\mathrm{H}}(r^\mu)$ for $\alpha = 1.25$ and $M = 0.1$ (left panel) and $M = 1$ (right panel).

We numerically evaluate $B_{\mathrm{H}}(r^\mu)$ in Eq. (17) for relatively large t and R and different values of α. In a wide regime of t and R the behaviour of $A_{\mathrm{H}}(r^\mu)$ is dominated by the term $M\,B_{\mathrm{H}}(r^\mu)$ in Eq. (16). Typical results are shown in Figs. 4 and 6 (a). The panel in Fig. 6 (b), showing the Dirac case $\beta = 1$, is reported for comparison. We assume different finite values for the mass M. The evolution of $B_{\mathrm{H}}(r^\mu)$ as the masses M are varied (for instance towards the limiting values predicted by the RG approach, see at the end of Section III) proceeds as follows. A rescaling $M \to a\,M$ does not change $B_{\mathrm{H}}(r^\mu)$ (up to a overall renormalization factor $a^{\frac{1-\beta}{\beta}}$) if the variables (t, R) are re-defined as

$$(t, R) \to (\tilde{t}, \tilde{R}) = (a\,t, a^{\frac{1}{\beta}}\,R)\,.$$

In this way the mass rescaling amounts to move on surfaces at constant values of the ratios $\frac{t}{R^\beta}$.

In Fig. 4, where each group velocity from the spectrum $E(p) = \sqrt{(p^\beta)^2 + M^2}$ is finite (at $\alpha = 1.75$, right panel), we see
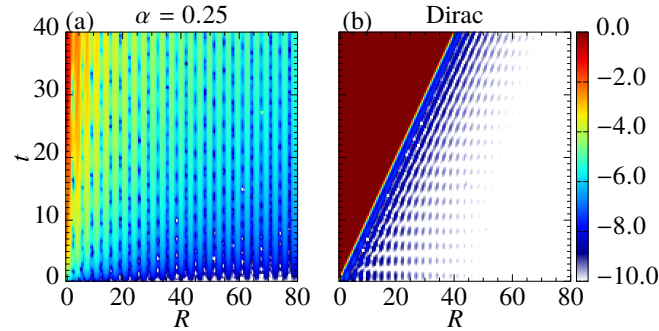

FIG. 6: Left panel: Plot of $B_{\mathrm{H}}(r^\mu)$ for $\alpha = 0.25$ and $M = 0.01$. Right panel: The same quantity in the Dirac case ($\beta = 1$) at $M = 1$.

connected regions with a form similar to a linear light-cone, from where some lobes departs. The multiple presence of the lobes suggests a scaling relation, depending on the ratio $\frac{t}{R^\gamma}$, for some γ function of α. The same scaling has been predicted on the lattice by an improvement of the bound in Eq. (10) derived in [6] and for continuous theories in [14]. Structures with similar scaling are also visible in the lattice calculations reported in the Subsection V (see e. g. Fig. 3).

Approximate conic profiles as in Fig. 4 occur in the entire range $\frac{3}{2} < \alpha < 2$, where the maximum velocity v_{max} stays finite. This finding agrees with the general expectation in previous works [14, 67, 77] and with [51]. In particular in [51] it has been stated that if $v_{max} < \infty$ the conic zones are the ones where a real solution k^* for the stationary-phase equation:

$$\left. \frac{\partial \lambda(k)}{\partial k} \right|_{k^*} = \frac{x}{t} \,. \tag{18}$$

can be found.

Interestingly enough, in Fig. 4 (left central and right central panels) the conic zones look bi-parted in two conic subregions. A better understanding of this phenomenon can be gained by analyzing the plots for $B_H(r^\mu)$ for fixed t and R varying. Typical situations are reported in Fig. 4, rightmost panel. There we see a finite region at small enough R where $B_H(r^\mu)$ is approximately constant, followed by an intermediate zone where the same quantity oscillates up to its maximum (the location of light-cone [51]), and by a region at larger R (outside of the light-cone) where the decay of $B_H(r^\mu)$ is algebraic. The extension of the first zone is linear in t, as suggested by the finiteness of the velocities itself, forming the first conic sub-region. Moreover the decay in the last zone appears in contrast with the exponential one predicted in [51], where however a *lattice* theory similar to Eq. (1) but with LR hopping has been considered. We consider an open and interesting question if the presence of conic sub-regions described above parallels the behaviour of the static correlation functions examined in [26], where two subleading decaying exponents terms, depending on M, have been derived analitically from the action S_{AN} in the regime $\frac{3}{2} < \alpha < 2$. Indeed, as visible in Fig. 5, if $\alpha < \frac{3}{2}$, then v_{max} diverges and these conic sub-regions disappear, as well as the mentioned exponentially decaying terms in the static correlations from S_{AN}.

If α decreases the correlation tends to spread on the space-time. In particular between $\alpha = 1.5$ and $\alpha = 1$, v_{max} diverges (paralleling the divergence on the lattice for the velocity of the singular modes) and the lobes tend to occupy all the space-time, forming structures similar to stripes. Nevertheless extended disconnected regions can be still found on the bottom of the panels (small t). Moreover, as said above, no conic regions are visible any longer. In this regime a calculation in stationary-phase approximation predicts $B_H(r^\mu)$ decaying as

$$B_H(r^\mu) \sim \frac{t^{\frac{1}{2(3-2\alpha)}}}{x^{\frac{2-\alpha}{3-2\alpha}}} \tag{19}$$

for large t and $\frac{R}{t}$. At variance, in the limits $t \to 0$, $R \to \infty$ and $M \to \infty$ (as implied by RG considerations, see Section III) the static-phase method gives for $B_H(r^\mu)$:

$$B_H(r^\mu) = f(M, t) \frac{1}{R^{2\alpha - 1}} \,, \tag{20}$$

with $f(M, t) = \frac{-1}{2M^2} \left[\frac{1}{M} \sin(Mt) - t \cos(Mt) \right]$. The power $2\alpha - 1$ also characterizes the asymptotical decay of the two fermions static correlations from S_{AN} in the same range for α, as expected by the formal similarity of the expressions for them with $A_H(r^\mu)$ [26].

For $\alpha < 1$, in correspondence with the divergent energy $\sqrt{(p^\beta)^2 + M^2}$ at $p \to 0$ (corresponding with the singular modes at $k \approx \pi$), the correlation is spread onto all the space-time (see Fig. 6 (a)), and no zone with vanishing $B_H(r^\mu)$ can be singled out, signaling an instantaneous propagation of information (even for diverging sizes of the simulated space-time). In the limit $t \to 0$ and $R \to \infty$ the static-phase method does not allow to evaluate the integral in Eq. (17) in this range. However we can readily observe that, in the large R limit, the major contributions to this integral come exactly from the momenta $p \to 0$ with diverging energy and from small time differences t. This fact suggests already a stronger deviation from relative locality, compared to the case $1 < \alpha < \frac{3}{2}$ [3, 10, 67]. We checked that the existence of the thin zone with vanishing correlation close to the line $t = 0$ in Fig. 6 (a) is a numerical effect, decreasing as the range of the numerical integration for $B_H(r^\mu)$ in Eq. (17) is increased.

In the case $\alpha > 2$, qualitatively correct results can be obtained neglecting since the beginning the RG subleading terms with odd integer p-powers in Eq. (7), then assuming an anomalous spectrum of the form $E(p) = \sqrt{(p + a(\beta) p^\beta)^2 + M^2}$. The term $\propto p^\beta$ is retained since it is crucial to reproduce the correct asymptotical behaviour for the static two points correlation functions from S_{AN}. Since RG arguments show that it also holds $a(\beta) \ll 1$ at $\alpha > 2$ [26], then the term $\propto p^\beta$ can affect $B(r^\mu)$ only quantitatively, apart from very large time and space separations. The resulting plot for $B(r^\mu)$, having $B_H(r^\mu)$ almost a Dirac form (see Eq. (17) with $\beta = 1$), effectively displays a clean (linear) conic connected region, in agreement with Fig. 3 (right panel). This result points to a weak deviation from the Lorentz locality when $\alpha > 2$, paralleling the weak violation of locality on the lattice found in the same range in the Subsection V.
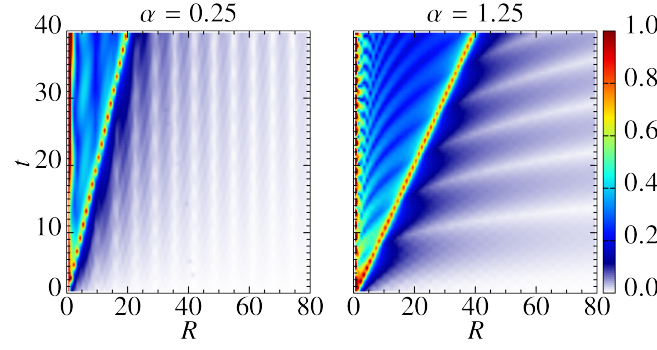
FIG. 7: Plots of $B(r^\mu) = B_L(r^\mu) + B_H(r^\mu)$ for $\alpha = 1.25$ and $M = 0.5$ (left panel) and for $\alpha = 0.25$ and $M = 0.01$ (right panel). In each point of the panels the values are again normalized with respect to the global maximum of the corresponding panel, so that the contributions of the light-cone get magnified.

Close to the line $\mu = -1$ and in the range $\alpha > 1$, where the ET for the LR paired Kitaev chain makes sense (see the Section III), the discussion proceeds very similar as above, in the light of the common form for the ET along the two critical lines $\mu = \pm 1$. In particular both when $1 < \alpha < 2$ and when $\alpha > 2$ all the main qualitative features as for the line $\mu = 1$ are reproduced, included the presence or the absence of a light-cone.

We notice at the end that similar studies on continuous theories have been performed on bosonic actions [67] and on an ET for the same lattice in Eq. (1), derived by a Landau-Ginzburg approximated scheme [74], and focusing on the range $\alpha > 1$ [14].

C. Discussion: lattice vs. effective results

All the results shown in Figs. 4-6 for the ET S_{AN} in Eqs. (7) and (8) are in good qualitative agreement with the lattice ones in Fig. 3 for large spatial separations R. In particular all the features related to nonlocality encountered in the lattice calculations are qualitatively reproduced. Quantitative differences in the magnitudes of $B_H(r^\mu)$ are mainly due to the (limited) role of the intermediate lattice excitations and to the chosen values for M in the Eqs. (7) and (8), a choice performed also following the RG prescriptions. This remarkable qualitative agreement strongly confirms the reliability of the ET in Eqs. (7) and (8) to describe the dynamics of the singular modes, also when the time evolution is concerned.

In spite of this agreement, the matching between the behaviours of $\Gamma(t, R)$ and $B_H(r^\mu)$ at small space separations is not completely satisfactory, especially at $\alpha < \frac{3}{2}$, since in the plots for the former quantity a linear light-cone, although approximate, is visible for every α, different from all the cases for $B_H(r^\mu)$. A closer look at Eq. (15) suggests that the mismatch can be solved adding to $B_H(r^\mu)$ the Dirac part $B_L(r^\mu)$. Indeed, as stated in Section III, this part describes the dynamics of the lowest energy lattice modes at $k \approx 0$, the same momentum where a peak in the velocity density $\rho(v)$ has been found and shown dominant for the non equilibrium dynamics of the LR paired Kitaev chain close to the line $\mu = 1$ [17].

Typical results obtained following this strategy are shown in Fig. 7. It is clear that now the mismatch between the results in Fig. 3 and Figs. 4-6 is solved, in a qualitatively satisfying manner and at every spatial separation, since the Dirac part $B_L(r^\mu)$ gives rise to a conic zone at small distances. The slope of the cone is fixed by the renormalized "light velocity" v_F appearing in the Dirac action S_D. Following the renormalization scheme in [26], this velocity equals its bare counterpart $v_F^{(0)}$. This quantity has been derived in Subsection V, Eq. (14).

A satisfying qualitative agreement is also achieved in the range $\alpha < 1$. However here the contributions out of the light-cone are more pronounced on the lattice, while at variance for the ET it is weakened by $M \to 0$ in Eq. (17), due to the intermediate modes in the lattice spectrum.

Summing up, we found that both for the lattice model in Eq. (1) and for the ET in Eq. (6) close to $\mu = 1$, at every α the dynamic correlations have two different behaviours, paralleling the static correlations. Indeed at fixed t there occur at small space separation a light-cone zone typical of SR lattice systems, and other regions at larger separations outside of the conic zone, related to the breakdown of locality by singular modes peculiar of the LR lattice model.

A summary of the main properties of the LR Kitaev model, also near the critical line $\mu = 1$, is presented in the Table I.

The situation is different close to the critical line $\mu = -1$, since, as mentioned in the previous Subsections, no light-cone is found for the ET in the range $1 \leq \alpha \leq 2$, different from the lattice case (see at the end of the Subsection V). The origin of the mismatch and of the difference with the case $\mu = 1$ relies on the fact that for $\mu = -1$ the velocity v_{emin} at the minima of the lattice energy spectrum ($k = \pi$) diverges, so that the singular modes coincides with the lowest energy ones and $\rho(v_{\mathrm{emin}}) = 0$: for these reasons no conic zone is observed in the ET, while the one occurring in the lattice calculations for $\Gamma(t, R)$ is related to a secondary peak in $\rho(v)$ [17].

property / α-range for α decreasing	$\alpha > 2$	$2 < \alpha < 3/2$	$3/2 < \alpha < 1$	$\alpha < 1$
conformal invariance ($\mu = 1$)	yes	no	no	no
area-law violation	no	no	no	yes
divergence in k-derivatives in $k = \pi$	$[\alpha]$	2	1	0
finite quasiparticle velocity	yes	yes	no	no
light-cone from the ET	yes	yes (+ corrections)	yes (+ stripes elongating towards infinity)	no (only for small R)

TABLE I: Summary of the properties for the LR paired Kitaev Hamiltonian in Eq. (1), as a function of α: a discussion of the comparison between the lattice model and the ET is presented in the text.

VI. GLOBAL QUANTUM QUENCHES

In this Section we investigate to what extent the (non-) causal structure analyzed in the previous Section for the dynamic correlation functions, deeply related to the action of the singular modes, can influence the non-equilibrium dynamics for the model in Eq. (1). We consider in particular the time evolution after global quenches and we work both at the lattice and the ET levels. Fixing the notation, let $|\psi_0\rangle$ be the ground state of the Hamiltonian H_0 before the quench and $|GS\rangle$ the ground state of the post-quench Hamiltonian H_1. In general $|\psi_0\rangle$ is a superposition of excited states for H_1, then the dynamics after the quenches is determined by the overlaps between $|\psi_0\rangle$ and them.

Considering general global quenches for the LR paired Kitaev chain in Eq. (1), both on the chemical potential, $\mu^{(0)} \to \mu^{(1)}$, and on the α exponent, $\alpha^{(0)} \to \alpha^{(1)}$, we have (for simplicity) at finite L:

$$|\psi_0\rangle = \prod_{n=0}^{L/2-1} \left(\alpha_{k_n}^{(0)} - i\beta_{k_n}^{(0)} a_{k_n}^\dagger a_{-k_n}^\dagger \right) |0\rangle \tag{21}$$

with $\alpha_{k_n}^{(0)} = \cos\theta_{k_n}$ and $\beta_{k_n}^{(0)} = \sin\theta_{k_n}$ having the same form as in Section III and the same expression with $\alpha_{k_n}^{(1)}$ and $\beta_{k_n}^{(1)}$ holding for $|GS\rangle$. From them it is easy to infer that the projection of $|\psi_0\rangle$ on $|GS\rangle$ reads

$$\langle\psi_0|GS\rangle = \prod_{n=0}^{L/2-1} \left(\alpha_{k_n}^{(0)}\alpha_{k_n}^{(1)} + \beta_{k_n}^{(0)}\beta_{k_n}^{(1)} \right) , \tag{22}$$

while the projections of $|\psi_0\rangle$ onto the excited eigenstates of H_1, having $2m$ Bogoliubov quasiparticles with m momenta opposite in pairs, read

$$a_{\{k_j\}} \equiv \langle\psi_0| \prod_{j=1}^{m} \{k_j, -k_j\}\rangle = i^m \prod_{j=1}^{m} \left(\alpha_{k_j}^{(1)}\beta_{k_j}^{(0)} - \beta_{k_j}^{(1)}\alpha_{k_j}^{(0)} \right) \prod_{p \neq j} \left(\alpha_{k_p}^{(0)}\alpha_{k_p}^{(1)} + \beta_{k_p}^{(0)}\beta_{k_p}^{(1)} \right) , \tag{23}$$

the symbol $\{j\}$ labelling the set of m pairs of opposite momenta. For future convenience we also report the quantity

$$\delta E \equiv \langle\psi_0|H_1|\psi_0\rangle - \langle GS|H_1|GS\rangle = \langle\psi_0|H_1|\psi_0\rangle = \sum_{k \in BZ} \lambda^{(1)}(k) |a_k|^2 \tag{24}$$

defining the difference between the (expectation values of the) energies, defined in terms of the post-quench Hamiltonian H_1, between $|\psi_0\rangle$ and $|GS\rangle$. The quantities a_k are defined in Eq. (23) (with a unique momentum considered), while $\lambda^{(1)}(k)$ are the quasiparticles energies from Eq. (2), the index α being omitted for sake of brevity.

A. Small quenches limit and validity of the ET

A notable consequence of Eq. (23) is that in the limit of small quench $\delta\theta = |\theta^{(0)} - \theta^{(1)}| \to 0$ (θ labelling the quench parameter, μ or α) only the overlaps between $|\psi_0\rangle$ and the two-particles states of H_1 is appreciably nonzero. We then examine in the same limit these overlaps for different values of $\mu^{(0)}$ and $\mu^{(1)}$. The results for $\alpha = 1.3$ are shown in Fig. 8. There it can be seen that, when H_1 is a critical Hamiltonian, $\mu^{(1)} = 1$ (left panel), for every α the overlaps between the pre-quench ground state and the post-quench excited ones is very peaked close to the minima of the final energy spectrum $\lambda_k^{(1)}$. This means that in the small quench limit only the modes (excited in pairs $\{k, -k\}$) close in energy to the post-quench ground state appreciably
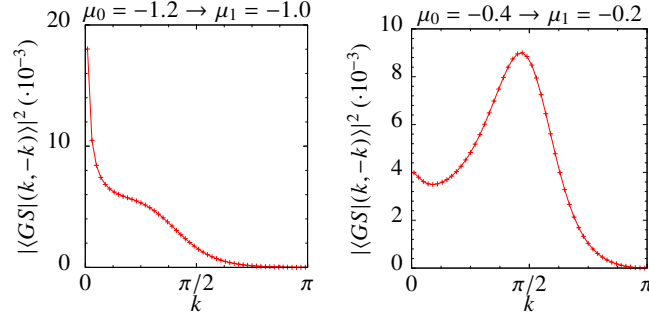
FIG. 8: Two-particle overlaps $\langle \text{GS}|\psi_0\rangle$ for two small quenches at fixed $\alpha = 1.3$ and respectively $\mu : -0.4 \to -0 - 2$ (left panel) and $\mu : -1.2 \to -1$ (right panel). In the latter case the maximum of the overlap coincides with the minimum of the energy. In the former instead the maximum is shifted, as a consequence of the nonzero mass gap of H_1.

contribute to the non-equilibrium dynamics of H_1. In this respect, we have that our LR system does not differ appreciably from the SR ones.

At variance, when H_1 is gapped (right panel), the maximum of the overlap does not coincide with the minimum of $\lambda^{(1)}(k)$: intuitively this is implied by the fact that in the small quench limit the energy difference δE between the ground states of H_0 and H_1 is vanishing, while the energy gap of H_1 is finite. The same result is not specific of the present model and setting, where $\mu^{(1)}$ is close to 1, but it holds whenever H_1 is gapped.

The observations above imply that, after a small quench to a critical point, the LR nature of the model can become appreciably manifest only when the singular modes are located close to the minima of the energy spectrum. Moreover a description of the post-quench dynamics in terms of the ET outlined in the Section III can work satisfactorily only in the same case. This is the case when $\mu^{(1)}$ approaches the semi-line $\mu = -1$ (with $\alpha > 1$), where the minimum of the energy spectrum coincides with the singular points, while the situation is different for the quenches approaching the critical line $\mu = 1$. This difference between the two critical lines parallels the difference seen in Section IV and concerning the agreement between dynamic correlations obtained on the lattice and from the ET close to the same lines. We notice however that also in the more favorable situation $\mu = -1$, the explicit ET calculations for the post-quench dynamics have still some subtleties that can spoil the agreement with the lattice ones, especially concerning the definition of the scaling limit for both the pre- and post-quench configurations, as outlined in [77].

B. Between small and large quenches

In the previous Subsection we investigated the limit of small quenches for the LR Kitaev chain. An opposite study has been performed in [17], where the limit of large quenches from $\mu^{(0)} \to \infty$ to $\mu^{(1)} = \pm 1$ has been considered. In this limit the overlaps between $|\psi_0\rangle$ and the excites states of H_1 are appreciably nonzero in every finite range of energies. For this reason, at least when the quasiparticle energy is limited, for $\alpha > 1$ (but, as we will see in a moment, also if $\alpha < 1$), the dynamics is mainly driven by the states whose density in velocity $\rho(v)$ displays peaks, a fact previously inferred in [9]. This observations suggests again a subleading effect of the singular modes for the time-evolution after a large global quench. Notably the large quench limit implies essentially the dynamics and the (non-) causality structure shown in the lattice calculations of Section IV: indeed there the action of space-dependent lattice operators a_i involves not negligible contributions by Bogoliubov quasiparticles having momenta in every part of the Brillouin zone.

It is interesting to analyze how the dynamics evolves interpolating between the small and large quench limits. For this purpose we introduce the following quantity:

$$I(v) = \frac{\rho(v)}{L} \left[\sum_{k \in \text{BZ}} \delta(v(k) - v) \sum_{m=0}^{\infty} \sum_{k_j \in \text{BZ}} |\langle \psi_0 | (k, -k) ; \prod_{j=1}^{m} {}' \{k_j, -k_j\} \rangle|^2 \right] \equiv \rho(v) W(v), \qquad (25)$$

being $|(k, -k) ; \prod_{j=0}^{m} {}' \{k_j, -k_j\}\rangle$ an eigenstate of H_1 with $2m+2$ Bogoliubov quasiparticles, a pair having momenta $\pm k$, and the other ones with momenta $\pm k_j$, k and k_j running on the positive part of the Brillouin zone. The prime index on the j-product means that $k_j \neq k$ and all the k_j are different each others (because of the Fermi statistics), while the function $\delta(v(k) - v)$ allows to count all the states with velocity v (notice indeed that $v(k) = \frac{\partial \lambda(k)}{\partial k}$ is not invertible in general).

The expression in Eq. (25) holds no matter the initial or the final values for μ and α and it expresses the weight of the (pairs of)

quasiparticles with velocity v for the post-quench dynamics, taking into account both a "kinematic" weight $\rho(v)$ and a "dynamic" weight $W(v)$ resulting from the possible superpositions of excited states involved in the dynamics after the quench.

The quantity $I(v)$ has, for a generic quench, the same role as $\rho(v)$ for large quenches, as the ones studied in [9, 17]. In particular it characterizes the spreading of the mutual information $J_{\{A,B\}}$ between disconnected parts of the chain A and B [78], setting for instance the natural time scales for it. In order to probe this statement, we consider first $I(v)$ in the small and large quench limits. In the first limit, as seen in the Subsection VI A, $\delta E \to 0$, then $I(v)$ reduces to:

$$I(v) = \frac{\rho(v)}{L} \left[\sum_{k \in \mathrm{BZ}} \delta(v(k) - v) |a_k|^2 \right], \tag{26}$$

a_k being defined as in Eq. (23) (with a unique momentum considered). Eq. (26) shows the importance to take into account the overlaps between $|\psi_0\rangle$ and the eigenstates of H_1, beyond the mere velocity density $\rho(v)$. Moreover it suggests that in the small quenches limit the role of $\rho(v)$ is hidden in general by the very low weights of the states with momenta not close to the minimum of the energy spectrum (see Fig. 8 and Subsection VI A). We then recover the suppression of the singular modes contribution seen in Subsection VI A.

Conversely, for large quenches (again here we consider conventionally μ varying) $I(v)$ behaves as follows. When the quasiparticle energies $\lambda(k)$ have all finite energy, $\lambda(k) \leq \lambda_{\max}$, if $\delta E \gg \lambda_{\max}$ (this is exactly the condition defining the large quench limit), then $W(v)$ tends to a constant, so that

$$I(v) \propto \rho(v), \tag{27}$$

and the result in [9, 17] is recovered. However, also when $\lambda_{\max} \to \infty$ (as for the LR Kitaev chain when $\alpha < 1$) the same conclusion is obtained, since for the excited states with diverging energy (coinciding with the singular modes in this case) it also holds $v \to \infty$, so that $\rho(v) \to 0$. The same consideration leads to conclude that, since the role of the singular modes is suppressed, also in the large quench limit the LR Kitaev chain does not differ appreciably from it SR counterpart, excepted for the possible appearance of secondary peaks in $\rho(v)$ at finite v [17]. Notably Eq. (25) is valid also in the SR limit $\alpha \to \infty$.

In [17] it has been argued that the suppression of the singular modes if their velocity diverges translates in a conic-like spreading for the mutual information $J_{\{A,B\}}$, although the system is strongly LR. Indeed deviations from this trend can be found smaller by various orders of magnitude. A similar situation is reported in Figs. 9 and 10, using a logarithmic scale for $J_{\{A,B\}}$.

Summing up, Eq. (25) provides a formal justification of the logic in [9, 17], using $\rho(v)$ to characterize the spreading of quantum correlations after global large quenches. Moreover it allows to link this limit with the small quench one.

A direct evaluation of $I(v)$ is difficult far from the small and large quench limits. However the continuous path between these limits can be followed considering again the behaviour of the mutual information $J_{\{A,B\}}$, as μ or α are varied in different ranges. An explicit example is reported in Figs. 9 and 10, where A and B are two disjoint sets of 16 sites, belonging to a chain with total length $L = 512$ and having varying relative distance R. We focus in particular on the evolution, as a function of the time t, after global quenches at fixed $\alpha^{(0)} = \alpha^{(1)} = 1.3$, ending up on the critical lines $\mu^{(1)} = \pm 1$ and starting from different values for $\mu^{(0)}$ such that $\delta\mu = \{0.2, 0.8\}$.

Our results explicitly show that when the quenches are relatively small, the relevant states for the spreading of the information are the ones close to the minimum of the energy spectrum, as stated in the Subsection VI A. In particular in the case $\mu^{(1)} = 1$ a dominant conic contribution, particularly pronounced on its edges, is found, in agreement with a peak in $\rho(v = v_{\mathrm{emin}} = v_F^{(0)})$ measured in [17] (v_{emin} is the velocity at the minimum of the energy, see Subsection V C). At variance, the role of the singular modes is negligible, also when v_{emin} diverges, since $\rho(v = v_{\mathrm{emin}}) \to 0$. This behaviour is clear in Fig. 9, where the mutual information is vanishing in the right-bottom zone of the panels. At variance, when $\mu^{(1)} = -1$, the spreading dynamics does not display any clear conic behaviour, and it is much slower than the previous case, since the effect of the lowest energy states, having here divergent velocity (the coinciding with the singular modes), is suppressed.

The differences between the two described situations parallels the different agreements found in Section IV between lattice and ET calculation for the dynamic correlations close to the critical lines.

When $\delta\mu$ increases, the contribution of the states far from the minima of the energy spectra (but having finite velocity) becomes more important. In particular when $\mu^{(1)} = 1$ the previous conic zone starts to enlarge, since a secondary peak becomes also relevant [17]. A similar situation occurs in the case $\mu^{(1)} = -1$, when the spreading dynamics become more rapid, again mainly thanks to the contribution of peaks at a finite v. In the large quench limit the cones related with the peaks in $\rho(v)$ get very pronounced on their edges and encode practically all the spreading for the mutual information. In this way one recovers the results in [17], also predicted by the discussion above regarding the functional $I(v)$ in Eq. (25).

We finally observe that the functional $I(v)$ can admit generalization to interacting lattice models. Indeed in these cases the time-scales for the evolution and for the spreading of information after a global quench are expected set by a functional similar to Eq. (26):

$$I(v) = \frac{\rho(v)}{N} \left[\sum_s \delta(v(s) - v) |\langle \psi_0 | s \rangle|^2 \right], \tag{28}$$

being N the total number of states for the system (possibly infinite) and $v(s) = \sqrt{\langle s|\hat{v}^2|s \rangle}$, with $\hat{v}^2$ the square velocity operator. We leave as an open question whether this functional generally implies a limited effect by the singular modes on post-quench dynamics, as for the LR paired Kitaev chain.
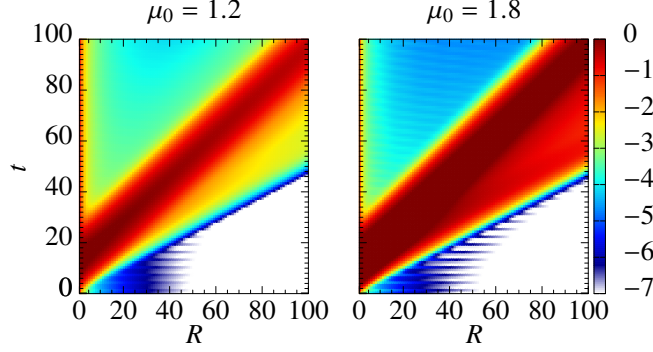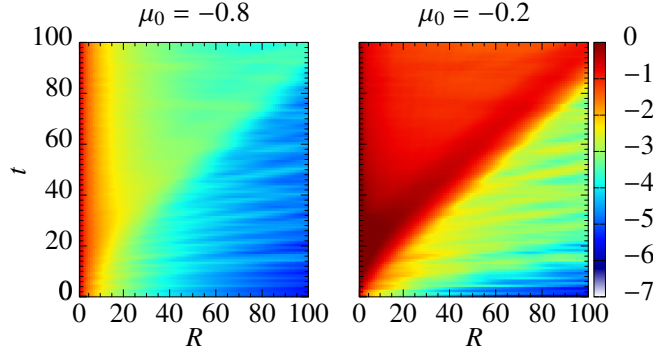

FIG. 9: Mutual information for quenches to the point with $\mu^{(1)} = 1$, $\alpha^{(0)} = \alpha^{(1)} = 1.3$ and initial values $\mu^{(0)} = 1.8$ (left panel) and $\mu^{(0)} = 1.2$ (rigth panel).

FIG. 10: Mutual information for quenches to the point with $\mu^{(1)} = -1$, $\alpha^{(0)} = \alpha^{(1)} = 1.3$ and initial values $\mu^{(0)} = -0.8$ (rigth panel) and $\mu^{(0)} = -0.2$ (left panel). In the second panel the magnitude of the mutual information on the edge of the cone rapidly increases with $\delta\mu$.

VII. CRITICAL BEHAVIOR, CAUSALITY AND NON-EQUILIBRIUM DYNAMICS IN THE PRESENCE OF LONG-RANGE INTERACTIONS

The results of the previous Sections allowed us to identify various interesting features of the equilibrium and non-equilibrium dynamics of the LR Kitaev chain. More in detail it has been outlined the central role played by the singular modes.

At this point is worth to investigate whether these features, or at least part of them, can be someway extended to some interacting LR models. In particular, from the discussion of the previous Sections on the LR Kitaev, which is a LR free fermionic model, it appears natural to conjecture that:

- the main differences, concerning both the equilibrium and non-equilibrium dynamics, between SR and LR systems are encoded in peculiar singularities/singular modes present in the second case. The set of singular modes can cover also the entire Hilbert space of the studied LR model. This possibility should hold for instance in the likely case that singularities are still manifest in the momentum space (canonically conjugated to the real space, where the singularities in the LR Hamiltonian terms primarily occur), since the momentum itself is no longer a good quantum number.

- the equilibrium dynamics at criticality for a LR system is governed both by the states close to the minimum of the energy and by the singular modes (having in general high energy compared to the first excited one). These latter states give rise to anomalous terms in the ET describing the critical points and they are eventually responsible for the breakdown of the conformal invariance, as well as for breakdown of the Lorentz invariance emerging at criticality for SR systems.

- both at the lattice level and for the critical ET, the singular modes are also responsible at every finite α of the algebraic decay tails of the static correlation functions, as well as for the appearance of non conic causally connected zones in the

dynamic correlation functions at large space separations (see Section IV). This feature is related with the violation of the LRB on the lattice and with the absence of Lorentz invariance for the ET. For the same reasons, in the ET description the causally connected zones are always reference frame dependent.

- close to the critical points an ET governing the equilibrium dynamics of a LR system can also work satisfactorily, at least qualitatively, for the temporal evolution after a small quench only if the singular modes occur isolated close to the minimum of the lattice energy spectrum, being in this way the unique states excited by a small quench.

To shed light on part of these open issues, in the following we present an investigation on the first three points, working on a paradigmatic interacting LR model, the LR Ising antiferromagnetic chain in Eq. (4).

A. LR Ising chain: singular dynamics from spin wave approach

In the deep paramagnetic ($\theta \approx 0$) or antiferromagnetic limits ($\theta \approx \frac{\pi}{2}$) a spin wave approach is reliable, at least qualitatively. For a review on this technique see e.g. [79, 80] and references therein. Theoretical studies in the spin wave approximation have been performed in the past both for static [18] and dynamic [3] correlation functions. In particular in [18] the hybrid decay of the static correlation functions has been derived by this approach. Moreover the causal structure of the Hamiltonian in Eq. (4) has been also probed experimentally in [46, 47], exactly analyzing the spin wave quasiparticle dynamics.

Here we reconsider dynamic correlation functions at different α in the deep paramagnetic limit at $\theta \to 0$ as in [3]. In this limit the Hamiltonian in Eq. (4) reduces in spin wave approximation to the quadratic Hamiltonian [19]:

$$H_{\mathrm{LRI,sw}} = \sum_k \left[a_k^\dagger a_k \, 2 \big(g_\alpha(k) \sin\theta + \cos\theta \big) + \big(a_k^\dagger a_{-k}^\dagger + a_k a_{-k} \big) g_\alpha(k) \sin\theta \right], \tag{29}$$

where k is the lattice momentum, a_k are bosonic operators related to the spin operators by Holstein-Primakoff transformation [79] and $g_\alpha(k) = \sum_{l=1}^\infty \frac{\cos(k\,l)\,(-1)^l}{l^\alpha}$. The bosonic Hamiltonian in Eq. (29) display several similarities with fermionic one in Eq. (3), with $\beta = \alpha$. It can be diagonalized again by (bosonic) Bogoliubov transformation, finding the spectrum

$$\bar\lambda_\alpha(k,\theta) = \sqrt{B(k,\theta)^2 - 4\,A(k,\theta)^2} \tag{30}$$

with $B(k,\theta) = 2\sin\theta\, g_\alpha(k) + 2\cos\theta$ and $A(k,\theta) = \sin\theta\, g_\alpha(k)$. Similar to the LR paired Kitaev chain around $\mu = 1$, the spectrum in Eq. (30) displays a minimum at $k = \pi$ and a momentum $k = 0$ where singularities develop in the derivatives of $\bar\lambda_\alpha(k,\theta)$. For instance from Eq. (30) we obtain that the expression for the quasiparticle velocity in the Brillouin zone, $v(k)$, diverges at $k = 0$ for $\alpha < 2$.

The Hamiltonian in (29) can be used to characterize the non-equilibrium dynamics in the paramagnetic limit, for instance after quenches on α at fixed $\theta \to 0$. In particular all the results in Section VI, included the overlaps in Eq. (22) and the quantity in Eq. (25), can be directly extended to this case.

In the same limit it is possible to reproduce, at least qualitatively, the dynamic correlation functions of the Hamiltonian in Eq. (4). To investigate the main features of them, similarly to what done in Section IV and using the Hamiltonian in Eq. (29), we compute the time-dependent commutator

$$\Gamma(t,R) \equiv \mathrm{Im} \left\langle \left[a_0, a_R^\dagger(t) \right] \right\rangle. \tag{31}$$

Numerical results are shown in Appendix B Fig. 14. There for every finite α we can see a double behaviour, as for the LR paired Kitaev chain: a connected conic zone at small space separations (compared to the ones in time) and another one, organized in stripes, extending outside of the cone, becoming more pronounced below $\alpha = 2$ (where the spin waves velocity diverges at $k = 0$) and eventually merging each others below $\alpha = 1$ (where the energy of the spin waves diverges at $k = 0$) [76]. These results are in agreement with the ones obtained in a recent paper [51], studying the parameter $\langle a_0(t) a_R^\dagger(t) \rangle$ after a global quench on the transverse field $\big($term $\propto \sigma^z$ in Eq. (4)$\big)$, and for the XXZ chain in [4]. We notice that qualitatively equal situation is expected for the LR Ising ferromagnetic chain in the deep paramagnetic limit, because of continuity.

Summing up, again the deviations from the SR picture (a purely connected zone related with the Lieb-Robinson bound) are found related with the singular modes, here at $k \approx 0$.

B. LR Ising chain: singular dynamics close to criticality

It is interesting at this point to investigate how the observed two-fold structure for locality evolves far from the paramagnetic limit and how singular dynamics finally affects the critical equilibrium behaviour of the LR Ising model. In this regime any
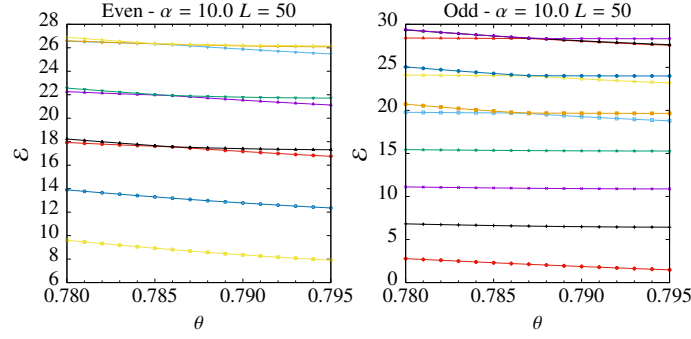
FIG. 11: Lowest energy levels around criticality for the antiferromagnetic Ising model at $L = 50$ and $\alpha = 10$, where the SR limit ($\alpha \to \infty$) is practically recovered. The left panel displays levels in correspondence with the family of the identity chiral operator ($\Delta = 0$), while the right one shows a similar correspondence with the family of the energy-density chiral operator ($\Delta = \frac{1}{2}$). The levels are organized in multiplets, with constant relative distances, as predicted by conformal invariance, and whose degeneracy at criticality ($\theta \approx 0.787$) is $1 - 1 - 2 - 2 - 3$ in the even sector (including the ground state at zero energy, not reported in the left panel) and $1 - 1 - 1 - 1 - 2 - 2 - 3$ in the odd sector.

non interacting approximations for that chain clearly fail, so that analitical predictions are not straightforward. However, a valid insight can be gained close to criticality analyzing the structure of the energy levels of the Hamiltonian in Eq. (4), as done in Section III for the LR Kitaev chain.

Results obtained from DMRG calculations with open boundary conditions, are reported in Fig. 12 for the LR antiferromagnetic Ising chain with $L = 50$ and $\alpha = 0.5$: these results have to be compared with the findings obtained in the SR limit (here considered reached at $\alpha = 100$) and plotted in Fig. 11. More in detail, the distribution of the energy levels, crossing at criticality ($\theta \approx 0.787$), is compared with the one predicted by the conformal theory proper of the SR Ising universality class (again with open boundary conditions) [81]. In particular the left panels in the two figures display the spin-flip Z_2 even sectors, while the right panels show the odd sectors. We recognize in the two panels of Fig. 12 the distributions the of energy levels respectively in correspondence with the family of the identity chiral operator ($\Delta = 0$) and with the family of the energy-density chiral operator ($\Delta = \frac{1}{2}$, Δ denoting the chiral weights), of the SR Ising conformal theory [81], also displayed in Fig. 11 (see details in the captions of Figs. 11 and 12).

These results suggest that the critical behaviour for the LR Ising model is similar to the one for the LR Kitaev chain at $\mu = 1$: for instance the critical exponents approaching this line are expected the same as for the SR Ising universality class [26]. However at the present time numerical limitations concerning the DMRG approach do not allow us to confirm this expectation.

More importantly, the breakdown of conformal symmetry, implied by the results in [19] and described in [21], must be due to the relevance at criticality of states far from the minimum of the energy spectrum. In this way, we find that the two-fold structure found in the paramagnetic limit, where singularities manifest in the derivatives of the (high energy) spectrum for the spin wave Hamiltonian in Eq. (29), survives also far from it, where interactions and quantum fluctuations are more important. The general necessity for LR critical systems to keep singular modes, in general with high energy, along the RG flow has been conjectured in [26]. The present case seems to reinforce this hypothesis, confirming also the relevance of a singular dynamics for various aspects of the LR systems, even interacting.

Accordingly, the correct ET for the LR Ising model is likely made by two terms, taking into account respectively of the lowest-energy states and the singular ones at higher energy scales, weakly coupled each others. For the same reason, we expect for this theory the same non Lorentzian causal structure seen in Subsection V B (the effect of the weak coupling being a mere perturbation, just affecting quantitative features of the theory).

We notice that the method used here and based on the study of distribution of the the lowest energy levels is rather general, being suitable for extension to other interacting LR models, even with higher dimensionality. Moreover it requires much limited sizes, compared to the method in [20, 21], where a finite-size scaling for the ground state energy density has been performed.

We finally mention that in literature a Landau-Ginzburg approximate Lagrangian exists for the ET describing the para-ferromagnetic quantum phase transition of the LR Ising chain [14, 74, 82]. It has been proposed for the ferromagnetic chain, but it is adoptable also for the antiferromagnetic one, the case considered in the present Section, after a proper definition of the order parameter: $m = \frac{1}{L} \sum_i (-1)^i \sigma_i^x$. The present study provides a justification a posteriori for the anomalous terms with fractional derivatives appearing in them. Moreover it suggests a similar scenario for other interacting models, also with continuous symmetries [16].
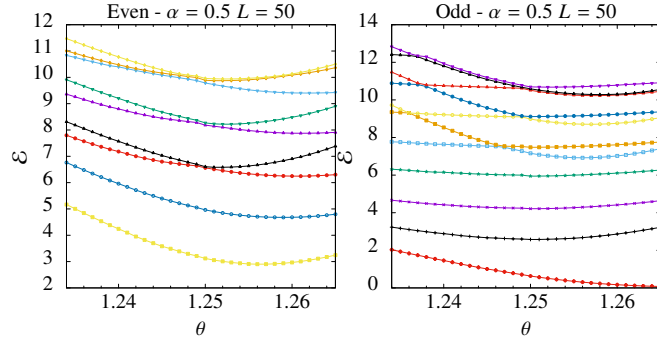
FIG. 12: Lowest energy levels around the critical point for the antiferromagnetic LR Ising chain at $\alpha = 0.5$ and $L = 50$, matching the typical distribution for the universality class of the critical SR Ising model, Fig. 11. Notice that, up to small finite size effects, the distances between the multiplets of levels is still constant at criticality, as required by conformal invariance. Moreover the crossing of the energy levels in every multiplet, identifying criticality ($\theta \approx 1.25$), agrees up to small finite size effects, generally occurring also in SR models, of the order $\Delta\theta \sim 10^{-3}$.

VIII.   CONCLUSIONS AND FUTURE PERSPECTIVES

In this paper we analyzed the locality breakdown in LR quantum models. Working at the beginning on a exactly solvable chain, the long-range (LR) paired Kitaev chain, we showed that both the static and dynamic correlation functions display, at every finite values for α, two different behaviours. The first one is common in short-range (SR) models while the second one is peculiar for LR systems (see also [8, 9]) and is due particular excitations, where the singularities coming from the long-rangeness of the model are encoded.

The same singular modes notably occur, with non trivial effects, at every finite α and even in the absence of divergences for the velocities or the energies of the excited lattice quasiparticles, a fact mostly underestimated in the previous literature. We showed that these excitations are responsible for the breakdown of locality, inducing violations from the Lieb-Robinson bound the lattice, as well as for the breakdown of conformal symmetry at criticality for small enough α. In turn, the breakdown of locality by the singular dynamics suggests for it a central role also concerning the violation of the Mermin-Wagner theorem in LR systems with continuous symmetries, see Section III.

The occurrence of nonlocal properties for $\alpha < 2$ has been studied in detail in the lattice theory. To illustrate the emergence of nonlocality in this regime we also introduced the effective theory (ET) in Eq. (8) which is nonlocal (as the lattice theory) and unitary. This is clearly different from what happens in the ET derived for SR models near criticality, which are local. We showed that the ET governs the equilibrium dynamics close to the criticality, and it is useful since it allows to conveniently single out and describe the action of the singular modes. In this theory the breakdown of locality manifests on the loss of the emerging Lorentz invariance for it, restored instead in the limit $\alpha \to \infty$. However, until when the maximum quasiparticle velocity stays finite, locality can be still defined in a weaker, reference frame dependent, way.

We checked that the ET allows for a qualitative agreement with lattice results for dynamic correlations provided that the contribution from the minima of the energy spectrum are also taken into account. The linear light-cone is found to be present, plus corrections (lobes or stripes) increasing when α is decreasing. For $\alpha < 1$ the ET gives a linear light-cone for small distances, while it is more clearly visible in the lattice results.

The role of the singular modes on the non-equilibrium dynamics after a global quench has been also analyzed, passing continuously from the small to the large quench limits. In the first limit the conditions posed by the singular modes for the reliability of the ET to describe the critical post-quench evolution are also discussed.

Finally we investigated the role of similar singularities on interacting LR models, focusing on the LR antiferromagnetic Ising model. In particular we found evidences for them in the deep-paramagnetic limit and strong clues also close to the critical points, where they deeply influence the critical dynamics. In both the cases apparently they interest excitations not close to the minima of the lattice energy spectrum, similarly as for the LR paired Kitaev chain at $\mu > 0$. In the light of these findings, the present study turns out to provide a justification a posteriori for the anomalous terms with fractional derivatives appearing in the approximate Landau-Ginzburg Lagrangians for the critical LR Ising model used e.g. in [14, 74, 82]. Moreover it suggests a similar scenario for other interacting models, also with continuous symmetries [16].

Main generalizations of the present work may concern the program begun on the LR Ising model, to reveal and to characterize the possible presence of singularities in other LR interacting systems, further clarifying how they affect their equilibrium and non-equilibrium dynamics and what they imply for the emergence of new symmetries and phases. In our opinion peculiar attention deserves the study (at least at the conceptual level) of systematic ways to construct of ET close to the critical points, encoding the possible LR singularities.

Most of the results discussed in the present paper are expected to be not be peculiar of one dimensional systems, and therefore an extension of our investigation to higher dimensional models appears highly interesting. Finally we notice that, due to the properties of nonlocality described in this paper, LR systems offer stimulating perspectives for the implementation of efficient quantum state transfer [83–85] and new classes of Kondo and Josephson devices (see e.g. [86–90]).

Acknowledgments

[1] A. Campa, T. Dauxois, D. Fanelli, and S. Ruffo, *Physics of long-range interacting systems* (Oxford, Oxford University Press, 2014).
[2] M. B. Hastings and T. Koma, Comm. Math. Phys. **265**, 781 (2006).
[3] P. Hauke and L. Tagliacozzo, Phys. Rev. Lett. **111**, 207202 (2013).
[4] J. Eisert, M. van den Worm, S. R. Manmana, and M. Kastner, Phys. Rev. Lett. **111**, 260401 (2013).
[5] D. Metivier, R. Bachelard, and M. Kastner, Phys. Rev. Lett. **112**, 210601 (2014).
[6] Z.-X. Gong, M. Foss-Feig, S. Michalakis, and A. V. Gorshkov, Phys. Rev. Lett. **113**, 030602 (2014).
[7] D. Damanik, M. Lukic, W. Yessen, and M. Lemm, Phys. Rev. Lett. **113**, 127202 (2014).
[8] M. Foss-Feig, Z.-X. Gong, C. W. Clark, and A. V. Gorshkov, Phys. Rev. Lett. **114**, 157201 (2015).
[9] D. M. Storch, M. van den Worm, and M. Kastner, New J. Phys. **17**, 063021 (2015).
[10] L. Cevolani, G. Carleo, and L. Sanchez-Palencia, Phys. Rev. A **92**, 041603(R) (2015).
[11] , L. Cevolani, G. Carleo, and L. Sanchez-Palencia, New J. Phys. **18** 093002 (2016).
[12] M. Kastner, New J. Phys. **17**, 123024 (2015).
[13] L. F. Santos, F. Borgonovi, and G. L. Celardo, Phys. Rev. Lett. **116**, 250402 (2016).
[14] M. F. Maghrebi, Z.-X. Gong, M. Foss-Feig, and A. V. Gorshkov, Phys. Rev. B **93**, 125128 (2016).
[15] T. Kuwahara, New J. Phys. **18** 053034 (2016).
[16] M. F. Maghrebi, Z.-X. Gong, and A. V. Gorshkov, `arXiv:1510.01325`
[17] M. Van Regemortel, D. Sels, and M. Wouters, Phys. Rev. A **93**, 032311 (2016).
[18] X.-L. Deng, D. Porras, and J. I. Cirac, Phys. Rev. A **72**, 063407 (2005).
[19] T. Koffel, M. Lewenstein, and L. Tagliacozzo, Phys. Rev. Lett. **109**, 267203 (2012).
[20] D. Vodola, L. Lepori, E. Ercolessi, A. V. Gorshkov, and G. Pupillo, Phys. Rev. Lett. **113**, 156402 (2014).
[21] D. Vodola, L. Lepori, E. Ercolessi, and G. Pupillo, New J. Phys. **18**, 015001 (2016).
[22] G. Gori, S. Paganelli, A. Sharma, P. Sodano, and A. Trombettoni, Phys. Rev. B **91**, 245138 (2015).
[23] F. Ares, J. G. Esteve, F. Falceto, and A. R. de Queiroz, Phys. Rev. A **92**, 042334 (2015).
[24] D. Giuliano, A. Sindona, G. Falcone, F. Plastina, and L. Amico, New J. Phys. **12**, 025022 (2010).
[25] J. Schachenmayer, B. P. Lanyon, C. F. Roos, and A. J. Daley, Phys. Rev. X **3**, 031015 (2013).
[26] L. Lepori, D. Vodola, G. Pupillo, G. Gori, and A. Trombettoni, Ann. Phys. **374**, 35 (2016).
[27] O. Viyuela, D. Vodola, G. Pupillo, and M. A. Martin-Delgado, Phys. Rev. B **94**, 125121 (2016).
[28] Z.-X. Gong, M. F. Maghrebi, A. Hu, M. L. Wall, M. Foss-Feig, and A. V. Gorshkov, Phys. Rev. B **93**, 041102 (2016).
[29] Z.-X. Gong, M. F. Maghrebi, A. Hu, M. Foss-Feig, P. Richerme, C. Monroe, and A. V. Gorshkov, Phys. Rev. B **93**, 205115 (2016).
[30] L. Childress, M. V. Gurudev Dutt, J. M. Taylor, A. S. Zibrov, F. Jelezko, J. Wrachtrup, P. R. Hemmer, and M. D. Lukin, Science **314**, 281 (2006).
[31] G. Balasubramanian, P. Neumann, D. Twitchen, M. Markham, R. Kolesov, N. Mizuochi, J. Isoya, J. Achard, J. Beck, J. Tissler, V. Jacques, P. R. Hemmer, F. Jelezko, and J. Wrachtrup, Nature Mater. **8**, 383 (2009).
[32] J. R. Weber, W. F. Koehl, J. B. Varley, A. Janotti, B. B. Buckley, C. G. Van de Walle, and D. D. Awschalom, Proc. Natl. Acad. Sci. **107**, 8513 (2010).
[33] M. Saffman, T. G. Walker, and K. Mölmer, Rev. Mod. Phys. **82**, 2313 (2010).
[34] S. Gopalakrishnan, B. L. Lev, and P. M. Goldbart, Phys. Rev. Lett. **107**, 277201 (2011).
[35] J. W. Britton, B. C. Sawyer, A. C. Keith, C.-C. J. Wang, J. K. Freericks, H. Uys, M. J. Biercuk, and J. J. Bollinger, Nature **484**, 489 (2012).
[36] P. Schauß, M. Cheneau, M. Endres, T. Fukuhara, S. Hild, A. Omran, T. Pohl, C. Gross, S. Kuhr, and I. Bloch, Nature **491**, 87 (2012).
[37] K. Aikawa, A. Frisch, M. Mark, S. Baier, A. Rietzler, R. Grimm, and F. Ferlaino, Phys. Rev. Lett. **108**, 210401 (2012).
[38] M. Lu, N. Q. Burdick, and B. L. Lev, Phys. Rev. Lett. **108**, 215301 (2012).
[39] C. Schneider, D. Porras, and T. Schaetz, Rep. Prog. Phys. **75**, (2012).
[40] B. Yan, S. A. Moses, B. Gadway, J. P. Covey, K. R. A. Hazzard, A. M. Rey, D. S. Jin, and J. Ye, Nature **501**, 521 (2013).
[41] O. Firstenberg, T. Peyronel, Q.-Y. Liang, A. V. Gorshkov, M. D. Lukin, and V. Vuletic, Nature **502**, 71 (2013).

[42] F. Dolde, I. Jakobi, B. Naydenov, N. Zhao, S. Pezzagna, C. Trautmann, J. Meijer, P. Neumann, F. Jelezko, and J. Wrachtrup, Nature Phys. **9**, 139 (2013).

[43] R. Islam, C. Senko, W. C. Campbell, S. Korenblit, J. Smith, A. Lee, E. E. Edwards, C.-C. J. Wang, J. K. Freericks, and C. Monroe, Science **340**, 583 (2013).

[44] A. Bermudez, T. Schaetz, and M. B. Plenio, Phys. Rev. Lett. **110**, 110502 (2013).

[45] E. Shahmoon and G. Kurizki, Phys. Rev. A **87**, 033831 (2013).

[46] P. Richerme, Z.-X. Gong, A. Lee, C. Senko, J. Smith, M. Foss-Feig, S. Michalakis, A. V. Gorshkov, and C. Monroe, Nature **511**, 198 (2014).

[47] P. Jurcevic, B. P. Lanyon, P. Hauke, C. Hempel, P. Zoller, R. Blatt, and C. F. Roos, Nature **511**, 202 (2014).

[48] J. S. Douglas, H. Habibian, A. V. Gorshkov, H. J. Kimble, and D. E. Chang, Nature Photon. **9**, 326 (2015).

[49] E. H. Lieb and D. W. Robinson, Comm. Math. Phys. 28, 251 (1972).

[50] G. Mussardo, *Statistical Field Theory: An Introduction to Exactly Solved Models in Statistical Physics* (Oxford, Oxford University Press, 2010).

[51] A. S. Buyskikh, M. Fagotti, J. Schachenmayer, F. Essler, and A. J. Daley, Phys. Rev. A **93**, 053620 (2016).

[52] I. S. Gradshteyn and I. M. Ryzhik, *Tables of Integrals, Series, and Products* (Amsterdam, Elsevier, 2007).

[53] M. Abramowitz and I. A. Stegun, *Handbook of Mathematical Functions* (New York, Dover, 1964).

[54] F. W. J. Olver, D. W. Lozier, R. F. Boisvert, and C. W. Clark, *NIST Handbook of Mathematical Functions* (Cambridge, Cambridge University Press, 2010).

[55] P. Fendley, J. Stat. Mech. P11020 (2012).

[56] A. Y. Kitaev, Phys. Usp. **44**, 131 (2001) [`arXiv:0110.440`].

[57] A. Dutta, G. Aeppli, B. K. Chakrabarti, U. Divakaran, T. F. Rosenbaum, and D. Sen, *Quantum Phase Transitions in Transverse Field Models* (Cambridge, Cambridge University Press, 2015).

[58] N. Defenu, A. Trombettoni, and A. Codello, Phys. Rev. E **92**, 052113 (2015).

[59] N. Defenu, A. Trombettoni, and S. Ruffo, Phys. Rev. B **94**, 224411 (2016).

[60] J. Sak, Phys. Rev. B **8**, 281 (1973).

[61] T. Horita, H. Suwa, and S. Todo, Phys. Rev. E **95**, 012143 (2017).

[62] P. di Francesco, P. Mathieu, and D. Senechal, *Conformal Field Theory* (New York, Springer, 1997).

[63] M. Henkel, *Conformal Invariance and Critical Phenomena* (New York, Springer, 1999).

[64] As explained in [50, 62], this fact is a straightforward consequence of the fermionic statistics of the Bogoliubov quasiparticles characterizing the excited levels and, more important, of the linear energy dispersion fulfilled by the lowest energy states.

[65] We point out that in the literature a further definition of locality is often given: a Lagrangian is defined local when it can be written as a functional $\mathcal{L}(x, \phi(x), \{\partial \phi^m(x)\})$ depending on a unique space-time coordinate x, on fields $\{\phi(x)\}$ and on a finite number of their integer derivatives [66]. For instance terms as $g(x,y)\phi(x)\phi(y)$ or as $\partial_x^l \phi(x)$, with l not integer, are forbidden. The action Eq. (8) is nonlocal also in this sense. However this definition of locality and the two previously introduced (validity Lieb-Robinson bound on the lattice and Lorentz locality in the continuous space-time) are in general not equivalent.

[66] S. Weinberg, *The Quantum Theory of Fields*, Vol. 1 (Cambridge, Cambridge University Press, 1995).

[67] M. A. Rajabpour and S. Sotiriadis, Phys. Rev. B **91**, 045131 (2015).

[68] M. F. Paulos, S. Rychkov, B. C. van Rees, and B. Zan, Nucl. Phys. B **902**, 246 (2016).

[69] F. J. Dyson, Comm. Math. Phys. 12, **91** (1969).

[70] H. Spohn and W. Zwerger, J. Stat. Phys. **94** 5 (1999).

[71] N. Defenu, P. Mati, I. G. Marian, I. Nandori, and A. Trombettoni, JHEP 1505(141) (2014).

[72] N. D. Mermin and H. Wagner, Phys. Rev. Lett. **17** 1133 (1966).

[73] M. Le Bellac, *Quantum and statistical field theory* (Clarendon Press, 1992).

[74] A. Dutta and J. K. Bhattacharjee, Phys. Rev. B **64**, 184106 (2001).

[75] M. E. Peskin and D. V. Schroeder, *An Introduction To Quantum Field Theory* (Reading, Addison-Wesley, 1995).

[76] Notice that the stripes outside of the light-cone in the upper parts of both the figures for $\alpha = 1.75$ and $\alpha = 1.25$ in Fig. 3 have opposite concavity compared to the stripes in the lower parts. However we checked that these lines vanish quite rapidly as the number of points evaluated to draw the pictures increases, so that only the lobes as in the lower regions of the panels remain. The same facts hold qualitatively for the spin wave analysis in Fig. 14.

[77] P. Calabrese and J. Cardy, Phys. Rev. Lett. **96**, 136801 (2006).

[78] V. Vedral, Rev. Mod. Phys. **74**, 197 (2002).

[79] H. T. Diep, *Frustrated Spin Systems* (Singapore, World Scientific, 2004).

[80] L.-P. Henry, P. C. W. Holdsworth, F. Mila, and T. Roscilde, Phys. Rev. B **85**, 134427 (2012).

[81] G. v. Gehlen and V. Rittenberg, J. Phys. A **19**, 631 (1986).

[82] S. Sachdev, *Quantum Phase Transitions* (Cambridge University Press, 2011).

[83] T. J. G. Apollaro, S. Lorenzo, A. Sindona, S. Paganelli, G. L. Giorgi, and F. Plastina, Phys. Scr. T165 014023 (2015).

[84] S. Bose and A. Bayat, *Quantum State Transfer and Network Engineering*, ed. G. Nikolopoulos and I. Jex (Springer, Berlin, 2013).

[85] Z. Eldredge, Z.-X. Gong, A. H. Moosavian, M. Foss-Feig, and A. V. Gorshkov, `arXiv:1612.02442`.

[86] D. Giuliano and P. Sodano, Nucl. Phys. B **770** 332-70 (2017).

[87] D. Giuliano and P. Sodano, Nucl. Phys. B **837** 153-85 (2010).

[88] B. Beri and N. R. Cooper Phys. Rev. Lett. **109** 156803 (2012).

[89] F. Buccheri, G. D. Bruce, A. Trombettoni, D. Cassettari, H. Babujian, V. E. Korepin, and P. Sodano, New J. Phys. **18** 075012 (2016).

[90] L. A. Landau, S. Plugge, E. Sela, A. Altland, S. M. Albrecht, and R. Egger, Phys. Rev. Lett. **116** 050501 (2016).

APPENDICES

Appendix A: Distribution of the energy levels at $\mu = -1$

We discuss in this Appendix the distribution of the lowest energy levels in the case $\mu = -1$, they are shown in Fig. 13. We see that, conversely to the case $\mu = 1$, this distribution does not agree with the one for the SR Ising model. Indeed the breakdown of the conformal symmetry for $\alpha < 2$ comes directly from the emergence of the non linear dispersion (actually inducing a singular group velocity) for the lowest energy Bogoliubov quasiparticles. The same dispersion deeply affects the distribution of the energy levels, as well as the critical exponents approaching the critical line, in the present case different in general from the ones proper of the SR Ising universality class.
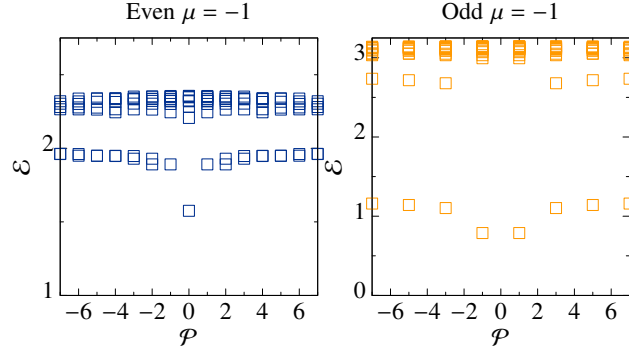
FIG. 13: Distributions of the lowest excited levels for the critical LR paired Kitaev chain for $\mu = -1$ and the same α of Fig. 1. As in Fig. 1 the left (right) panel shows the sector with an even (odd) number of quasiparticles, while the doubly degenerate levels are marked by a double square. It is clear that the obtained levels, found for the critical LR paired Kitaev chain at $\mu = 1$ and typical of the SR Ising universality class, cannot be recovered in the present case. Moreover no constant energy difference is found between the various multiplets. These facts underline the loss of the conformal invariance for the lowest energy states of the critical LR paired Kitaev chain at $\mu = -1$.

Appendix B: Dynamic correlations for the spin wave Hamiltonian in Eq. (29) of the main text

We plot in this Appendix, in Fig. 14, the time-dependent commutator

$$\Gamma(t, R) \equiv \text{Im} \left\langle \left[a_0, a_R^\dagger(t) \right] \right\rangle = \frac{1}{2\pi} \, \text{Im} \int \mathrm{d}k \, \mathrm{e}^{\mathrm{i}kR} \left[\mathrm{e}^{\mathrm{i}\bar{\lambda}_\alpha(k,\theta)t} + 2\mathrm{i}|\beta(k,\theta)|^2 \sin \left(\bar{\lambda}_\alpha(k,\theta)t \right) \right], \tag{B1}$$

where $\beta(k, \theta) = \sqrt{\dfrac{B(k,\theta)}{2\,\bar{\lambda}_\alpha(k,\theta)} - \dfrac{1}{2}}$. The discussion of the plotted results is in the main text.
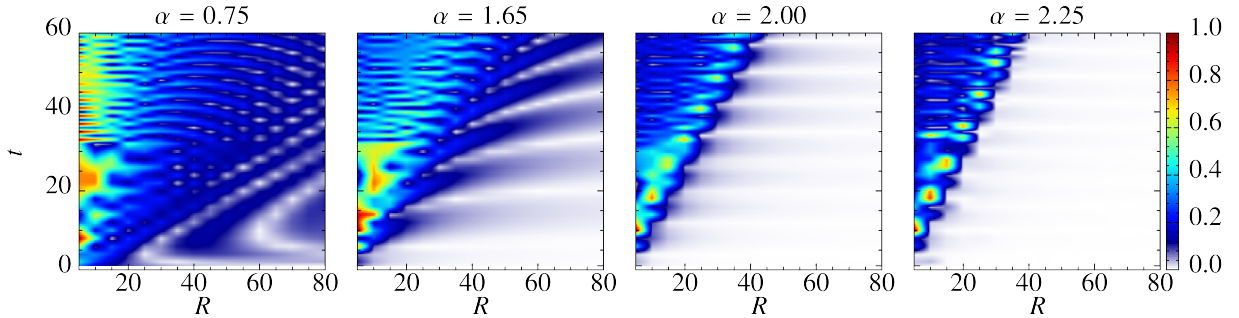
FIG. 14: Plots of $\Gamma(t, R)$ in Eq. (B1) for (from the right hand side) $\alpha = 2.25$, $\alpha = 2$, $\alpha = 1.65$, and $\alpha = 0.75$. The stripes with negative concavity outside the cone appear to have the same nature and trend as the ones for the LR paired Kitaev chain $\big($Eq. (1) of the main text$\big)$ in the same regimes for α, see the note [76] referring to Section V.